Journal of Bionanotechnocracy: Countdown to 2030

Investigating Hidden Science, Emerging Technologies, and Suppressed Truths

Crystal–Fibre Assemblies Across Domains
Recurrent Phase-Coupled Structures in Pharmaceuticals and Biological Fluids

David Nixon, M.B., Ch.B.
Independent Scholar and Physician
Brisbane, Australia

Email: david@drdavidnixon.com | Website: www.drdavidnixon.com |ORCID: 0009-0007-9817-5421

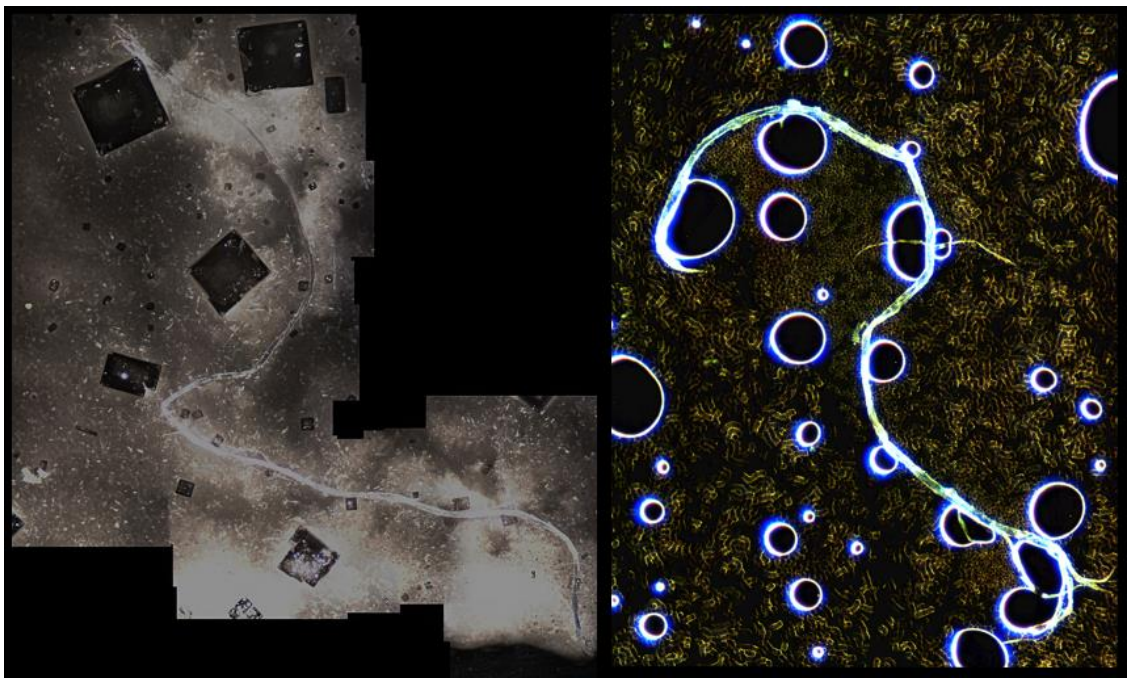

Contents

Acknowledgements

I thank Xstra Technologies Group and the subscribers of the NixonLab Substack for their support and contributions to this research. I also wish to make special acknowledgement of Professor Wendy Hoy FAA AO FRACP, Emeritus Professor of Medicine at the University of Queensland, whose support extended well beyond academic encouragement, and whose personal integrity, clinical insight, and steadfast presence during challenging periods made this work possible.

The following individuals contributed microscopy images, observational insights, and collaborative discussion that supported the development of this work. All interpretations, analysis, and conclusions remain the responsibility of the author.

Unhackable Animal
Tobias Beharrell
Louise Coats
Gideon Jacobs
Carol Magee
Jeff Miller
Will Wade

Journal of Bionanotechnocracy: Countdown to 2030

Investigating Hidden Science, Emerging Technologies, and Suppressed Truths

Crystal–Fibre Assemblies Across Domains
Recurrent Phase-Coupled Structures in Pharmaceuticals and Biological Fluids

David Nixon, M.B., Ch.B.
Independent Scholar and Physician
Brisbane, Australia

Email: david@drdavidnixon.com | Website: www.drdavidnixon.com |ORCID: 0009-0007-9817-5421

Abstract

Across multiple independent microscopy-based investigations, a recurring structural motif has been observed in diverse pharmaceutical preparations and biological fluids: a coupled architecture in which crystalline domains are directly associated with fibrous or filamentous elements. These structures, designated here as Crystal–Fibre Assemblies (CFAs), exhibit organised geometry, persistence across phase transitions, and responsiveness to environmental context. CFAs have been identified in dental and non-dental anaesthetics, vaccine suspensions, and biological samples including blood and urine.

CFAs are defined not by chemical composition but by architectural relationship. Their defining feature is a reproducible spatial coupling between crystalline phases and fibre-like structures, frequently characterised by nodal junctions, directional growth, and vesicle-associated dynamics. The recurrence of this motif across chemically and biologically distinct domains argues against contamination or isolated formulation artefacts and instead points to shared phase-contingent organisational logic operating at the interface between nanoscale organisation and microscale structure.

This study does not seek to assign definitive mechanistic causation or biological function. Rather, it establishes CFAs as a reproducible structural motif whose cross-domain appearance warrants consideration within a soft-matter and systems-theoretic framework. When the same architecture emerges in unrelated contexts, the interpretive focus shifts from compositional identity to the physical conditions that permit its formation, suppression, or redirection. The results presented delineate where CFAs reliably arise, where they are constrained, and what these boundary conditions reveal about phase-coupled organisation in complex fluids.

Keywords:

phase-dependent transformation; crystal–fibre assemblies (CFA); soft-matter organisation; dark field microscopy; non-classical crystallisation; fibre formation; mesoscale dynamics; structural classification

General Audience Summary

Across many microscope studies, the same unexpected pattern appears again and again: crystals physically linked to fibres in an organised way. These formations, called Crystal–Fibre Assemblies (CFAs), have been observed in dental anaesthetics, vaccine preparations, other injectable pharmaceuticals, and biological fluids such as blood and urine.

What makes CFAs notable is not what they are made of, but how they are organised. In each case, a crystalline structure is directly connected to one or more fibres, often showing clear geometry and persistence even when conditions change. The appearance of the same structure in chemically unrelated materials makes simple contamination or chance artefact unlikely.

Instead of focusing on composition, this study asks under what conditions such organised forms emerge. By comparing where CFAs appear — and where they do not — the findings suggest they reflect a recurring organisational logic at the boundary between crystalline and fibrous phases, pointing to broader principles governing structure and stability in complex fluids.

Introduction

Across multiple independent lines of microscopy-based observation, a recurring structural motif has emerged: coupled crystalline and fibrous assemblies exhibiting organised geometry, persistence across phase transitions, and responsiveness to environmental context. These structures, referred to here as *Crystal–Fibre Assemblies (CFAs)*, have been observed in pharmaceutical preparations, dental anaesthetics, non-dental anaesthetics, and biological fluids, including blood and urine.

CFAs are not defined by chemical composition alone. Rather, they are characterised by a distinctive architectural relationship between crystalline domains and fibre-like elements. These assemblies often exhibit nodal junctions, directional growth, and vesicle-associated dynamics. Their recurrence across chemically and functionally distinct materials suggests that they arise not from contamination or isolated formulation artefacts, but from shared phase logic operating at the interface between nanoscale organisation and microscale structure.

The purpose of this paper is not to catalogue every instance of CFA occurrence, nor to assign definitive mechanistic causation. Instead, it aims to establish CFAs as a reproducible structural motif whose appearance across domains warrants serious consideration within a soft-matter and systems-theoretic framework. When the same architecture appears in unrelated contexts, the question shifts from what is it made of to what conditions allow it to form.

Across all examined samples, a recurring structural motif is observed in which crystalline domains are directly coupled to fibrous or filamentous elements. This configuration is here designated the Crystal–Fibre Assembly (CFA). The defining feature of a CFA is not chemical composition, but architectural relationship: a persistent spatial and functional linkage between a crystalline phase and one or more fibre-like structures.

The term *Crystal–Fibre Assembly (CFA)* was first introduced in an earlier microscopy-based analysis of pharmaceutical samples to describe this recurring coupled crystal–fibre architecture. It is retained here for continuity and to distinguish the motif from generic crystallisation or isolated fibre formation.

CFAs typically present as planar or polyhedral crystalline bodies from which fibres emerge, intersect, or terminate at crystal boundaries. In many instances, fibres appear to act as anchoring elements, alignment guides, or conduits for subsequent structural growth. The crystal and fibre components do not appear randomly associated; rather, their geometry suggests coordinated formation or mutual stabilisation.

This motif is observed across diverse contexts, including dental anaesthetics, vaccine suspensions, non-anaesthetic pharmaceuticals, blood, and urine samples. While absolute morphology varies between domains, the core relationship — crystal continuity coupled

to fibrous architecture — remains conserved. This recurrence across chemically and biologically distinct environments supports classification of the CFA as a structural motif rather than an artefact of a single formulation or preparation method.

Importantly, CFAs are observed to persist across phase transitions, including drying, dilution, and rehydration, indicating a degree of phase stability inconsistent with transient crystallisation alone. Their repeatability across samples and conditions suggests an underlying organisational logic operating at the interface between crystalline and fibrous phases.

To avoid ambiguity and over-classification, the term Crystal–Fibre Assembly (CFA) is used in this paper only when a structure meets the explicit inclusion criteria defined below.

Inclusion Criteria: What Constitutes a Crystal–Fibre Assembly

For the purposes of this analysis, a structure is classified as a Crystal–Fibre Assembly (CFA) when it satisfies the following criteria:

Coupled architecture
A direct and spatially coherent association between a crystalline domain and one or more fibre-like elements must be present. Proximity alone is insufficient; the components must appear structurally linked or mutually stabilised.

Geometric organisation
The crystalline component exhibits defined geometry (planar, rectilinear, polyhedral, or modular), while fibres display directional growth, anchoring, or nodal attachment rather than random dispersion.

Persistence across conditions
The assembly remains identifiable across changes in phase or context, including drying, dilution, incubation, or partial disassembly. Transient crystallisation without persistence does not qualify.

Reproducibility across samples
Comparable architectures are observed in independent samples or domains, ruling out single-sample artefacts or preparation-specific anomalies.

Only structures meeting all four criteria are designated CFAs in this paper.

What CFAs Are Not: Excluded Artefacts and Misclassifications

CFAs are explicitly distinguished from several common microscopic phenomena:

Isolated crystals
Crystalline structures lacking any consistent fibre association, even when geometrically complex, are not classified as CFAs.

Free fibres or filaments
Fibrous elements without crystal coupling, including amorphous strands, proteinaceous threads, or drying artefacts, are excluded.

Preparation artefacts
Edge effects, coverslip pressure distortions, air–liquid interface artefacts, and contamination introduced during slide preparation do not meet CFA criteria unless the coupled architecture persists beyond the preparation context.

Random aggregation
Clusters formed through passive sedimentation or non-specific agglomeration, lacking organised geometry or repeatable form, are excluded.

This exclusion framework is essential to preserve CFAs as a structurally meaningful designation rather than a catch-all term.

Minimal Taxonomy of Crystal–Fibre Assemblies

While CFAs exhibit morphological diversity, observed instances can be provisionally grouped into three recurrent classes:

Type I: Anchored CFAs
Fibres terminate at or emerge from discrete points along a crystalline boundary, suggesting anchoring or nucleation roles.

Type II: Embedded CFAs
Fibres traverse or are partially enclosed within the crystalline domain, often associated with internal compartments or nodal inclusions.

Type III: Networked CFAs
Multiple crystal–fibre units are linked into larger assemblies through shared fibres or nodal junctions, forming lattice-like or modular networks.

This taxonomy is descriptive rather than mechanistic. Its purpose is to support comparative analysis across domains and to facilitate recognition of conserved architectural patterns.

Occurrence Across Domains

Crystal–Fibre Assemblies (CFAs) have now been observed across multiple material domains, including pharmaceutical preparations, biological fluids, and environmental samples. Their recurrence in chemically and procedurally distinct contexts argues against a domain-specific artefact and instead supports the interpretation of CFAs as a reproducible structural motif arising under shared physical conditions.

In pharmaceutical samples, CFAs have been documented in mRNA vaccines (including Pfizer–BioNTech and Moderna formulations), dental anaesthetics such as prilocaine, and other injectable preparations. In these contexts, CFAs appear as crystalline domains structurally coupled to fibrous or filamentous elements, often exhibiting organised geometry, internal inclusions, and sharp phase boundaries. Importantly, these assemblies are observed directly within unopened or freshly prepared pharmaceutical samples, eliminating explanations based on biological excretion or environmental contamination.

Comparable architectures have also been identified in biological fluids, including blood and urine. In these samples, CFAs frequently present as fibre-centred crystalline growths with lobed or radial morphology, sometimes embedded within or adjacent to proteinaceous or gel-like matrices. While the biochemical environments differ substantially from pharmaceutical preparations, the underlying structural logic — fibre–crystal coupling, phase stability, and geometric regularity — remains consistent.

The appearance of CFAs across these domains suggests that their formation is governed less by specific chemical composition and more by shared physical or mesoscale conditions, such as phase transitions, coherence domains, or field-responsive self-assembly processes. Notably, the same motif has been observed under different microscopy techniques and preparation methods, further reducing the likelihood of procedural artefact.

Crucially, the presence of CFAs in both biological and non-biological contexts reframes the interpretive question. Rather than asking what substance the structures are composed of, the more productive inquiry becomes under what conditions such architectures reliably emerge. This shift from compositional identity to structural behaviour aligns with

a soft-matter and systems-theoretic framework, in which organised morphology can arise from dynamic interactions between materials, fields, and boundary conditions.

Taken together, these observations indicate that Crystal–Fibre Assemblies represent a recurring structural phenomenon spanning domains traditionally treated as separate. Their consistent appearance across pharmaceutical preparations and biological fluids suggests an underlying physical logic governing phase-coupled organisation, rather than isolated anomalies tied to composition or preparation. This study therefore examines CFAs as phase-contingent outcomes within soft, responsive material systems, with particular attention to the conditions under which crystallisation is permitted, suppressed, or redirected. The Results that follow focus on observational convergence, divergence, and boundary conditions, rather than frequency alone.

The Results section therefore focuses on observational convergence, divergence, and exception, rather than frequency alone.

Methods

Microscopy

Neogenesis System 9W LED Microscope

This system was equipped with an HDFMI-compatible HD USB camera (maximum resolution 3264 × 1836). It featured interchangeable condensers:

- Brightfield condenser: Abbe condenser with frosted filter (NA 1.25)
- Dark field condenser: Oil immersion cardioid condenser

Slide Preparation

- Manufacturer: Livingstone International Pty Ltd
- Dimensions: 76.2 × 25.4 mm; thickness: 0.8–1.0 mm
- Cleaning: Sterile 70% isopropyl alcohol swab; dried with Kimtech™ wipers

Sample Handling and Preparation

Samples were imaged without chemical fixation, staining, or dehydration. Fluids were transferred directly to cleaned glass slides and observed primarily under dark field microscopy within minutes to hours of preparation. Coverslips were used only where required to achieve higher magnification objectives and were not employed to induce structural change. In all cases, the dominant organising process was sessile droplet evaporation (SDE). Where noted, complementary bright field imaging was used to confirm morphology. No external reagents were added, and no attempt was made to induce crystallisation; observed structures emerged spontaneously under the conditions described.

Additional images were contributed by independent collaborators using comparable optical microscopy systems capable of dark-field and phase-contrast imaging at magnifications between 40× and 400×. While specific hardware configurations varied, all systems shared equivalent optical constraints relevant to the observations described.

Results

Among the more distinctive CFA configurations observed in the Pfizer-BioNTech formulation were compound crystalline assemblies linked by soft, curving filaments. These appeared early in the sample lifecycle and consistently exhibited structured symmetry, with rectangular and trapezoidal plates coupled by branching or daisy-chain fibre networks. The geometry, spacing, and interconnectivity implied active assembly behaviour rather than incidental aggregation.

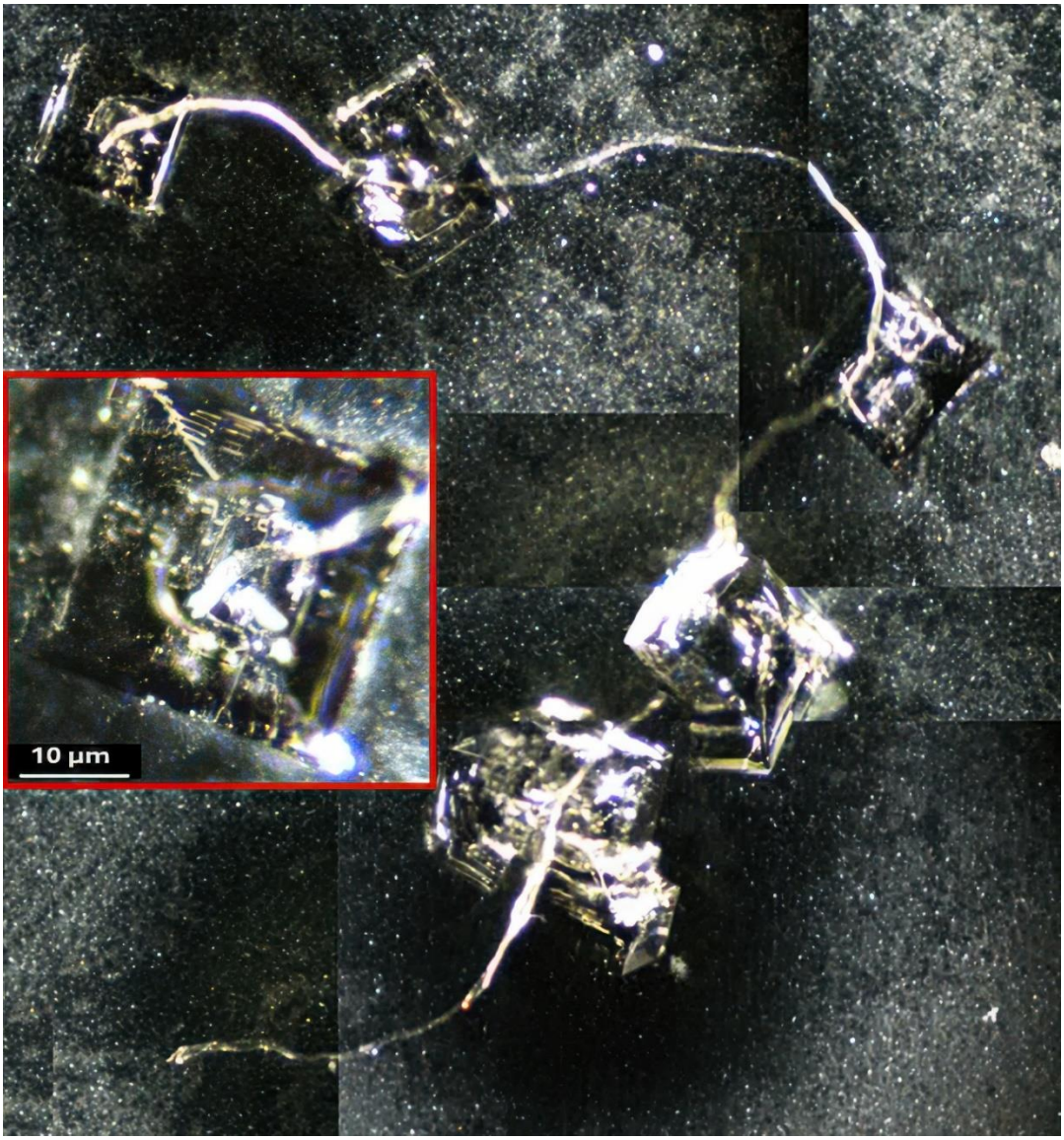

Figure 1. Figure 1. Early CFA network ("daisy chain") in Pfizer-BioNTech Comirnaty, showing crystal-to-fibre links and nodal complexity. Inset: high-magnification view with scale (10 µm)

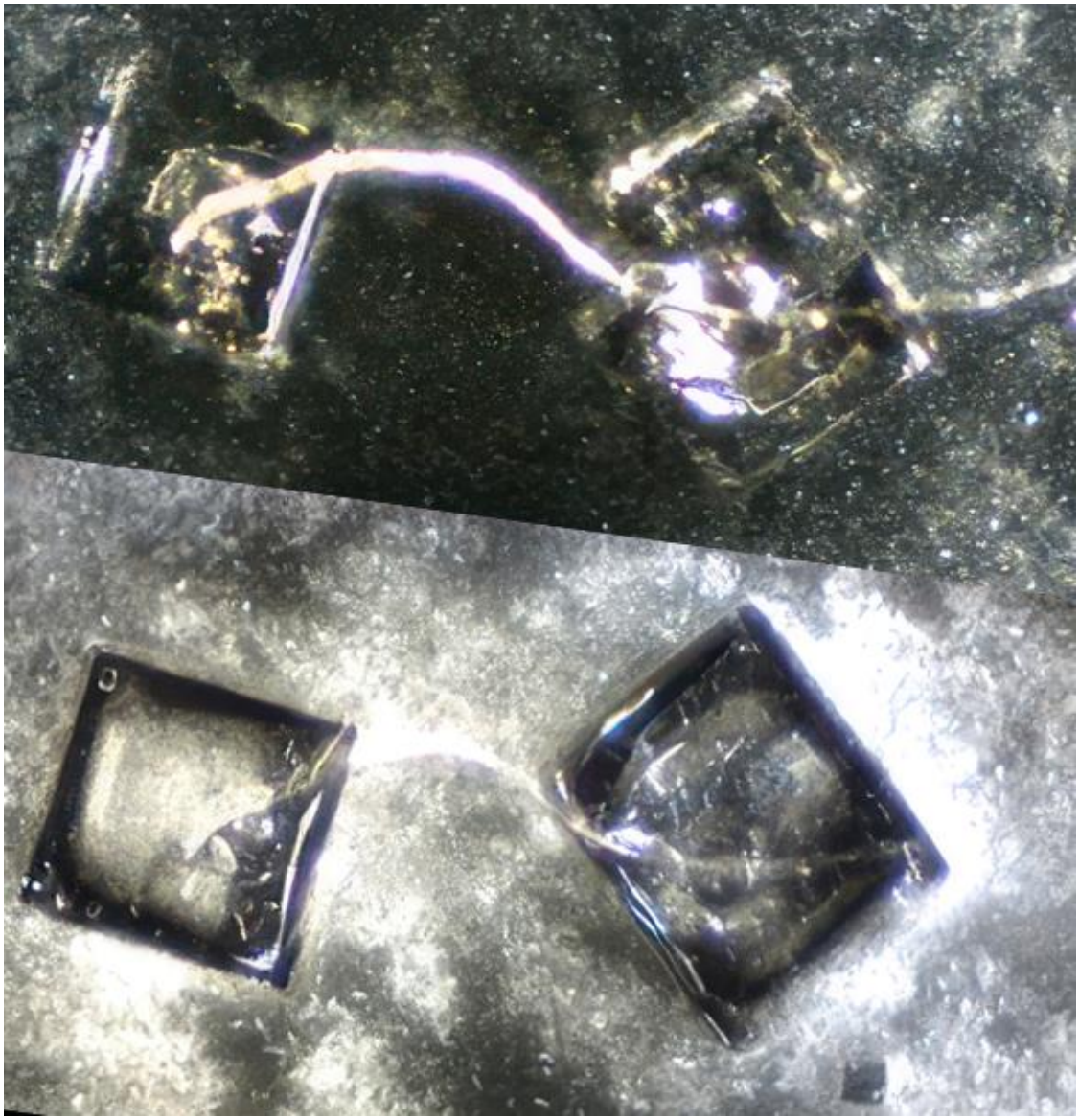

Figure 2. CFA structure imaged two months apart under identical magnification and matched orientation. Top: early-stage presentation with partially resolved boundaries, fibre attachment, and irregular internal topography. Bottom: same assembly after two months under ambient storage, now exhibiting full geometric resolution, sharp edge articulation, and stable inter-fibre connectivity. Magnification 200x.

This time-lapse pairing makes the developmental logic of the CFA system unmistakable. Both crystals, initially blurred and fragmented, advance into well-formed square geometries with consistent edge thickness, distinct internal domains, and what appear to be corner anchor points. The interlinking fibre not only persists but retains spatial memory of its arc, suggesting that the structure as a whole is not simply stable but actively

self-stabilising. Such maturation over time—absent any external stimulus—reinforces the hypothesis that these are not transient precipitates, but latent architectural systems, governed by field-responsive logic, coherence dynamics, or soft templating mechanisms embedded within the formulation itself.

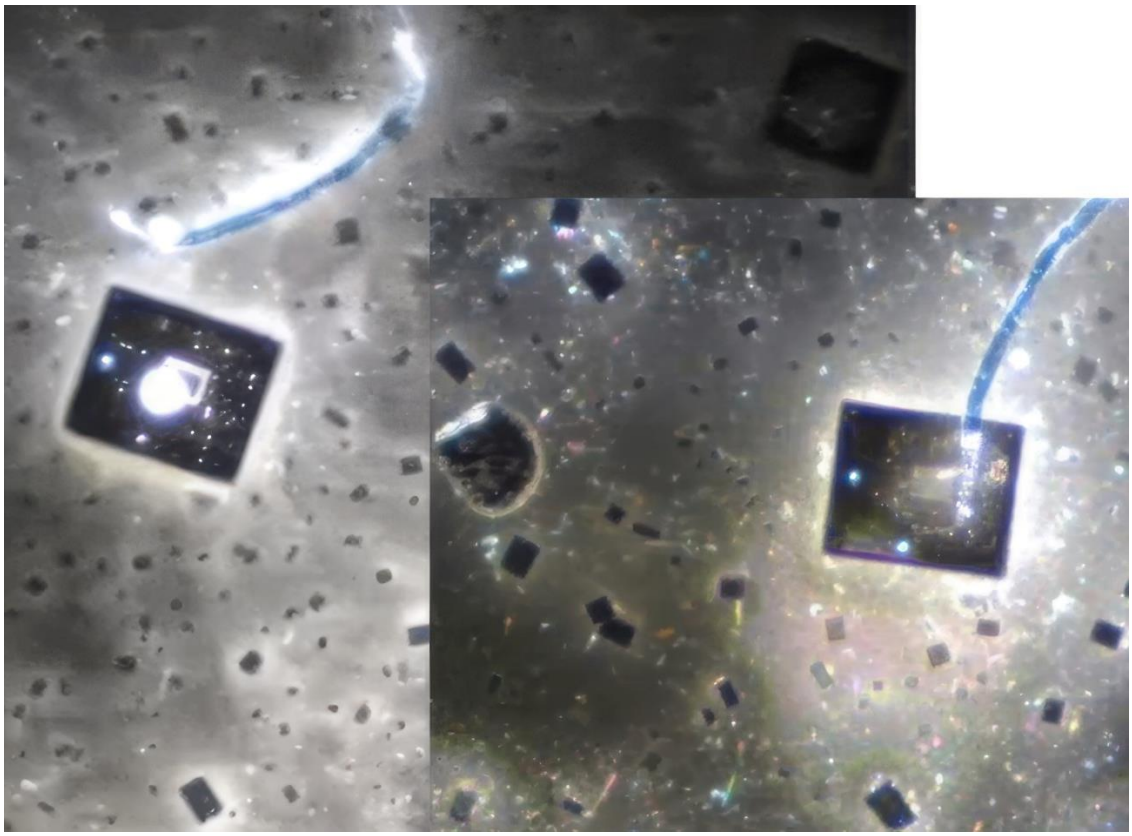

Figure 3. CFA node in Pfizer-BioNTech Comirnaty shown across two timepoints. A single square crystal, connected to a flexible blue fibre, is embedded in a field of smaller rectangular microforms. Left: initial state, with disordered scatter of microforms. Right: same region two days later, showing increased spatial regularity and local alignment within the field, while the anchor structure remains unchanged. No external stimulus applied. Magnification 100x.

Figure 4. Overlay of two time-separated images showing evolution of a CFA crystal in Pfizer-BioNTech Comirnaty. The crystal has rotated and translated slightly; however, a blue fibre appears in the later image with no precursor structure in the earlier frame. Its position, arc, and entry point suggest either 3D emergence, delayed assembly, or structural insertion — none of which are easily explained by conventional crystallisation or passive phase dynamics.

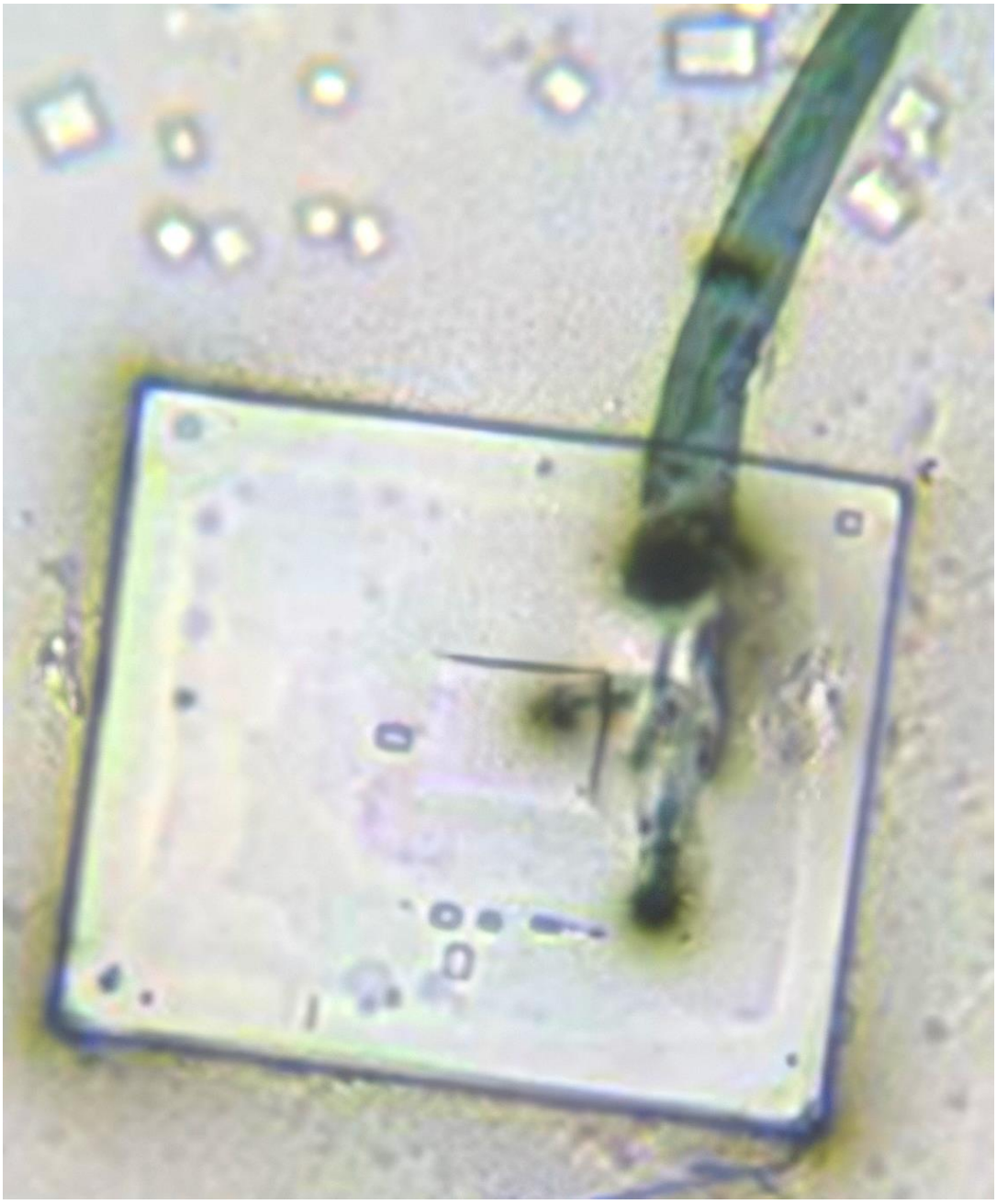

Figure 5. Bright field micrograph of a CFA node in Pfizer–BioNTech Comirnaty, showing a square crystal with distinct internal patterning and a vertically oriented fibre attached at the junction socket. Multiple anchoring points are visible, including circular and oval nodes, suggesting engineered coherence or functional design. The clarity of edges and embedded symmetry supports interpretation of this structure as part of an integrated crystal–fibre assembly. Magnification ~400x.

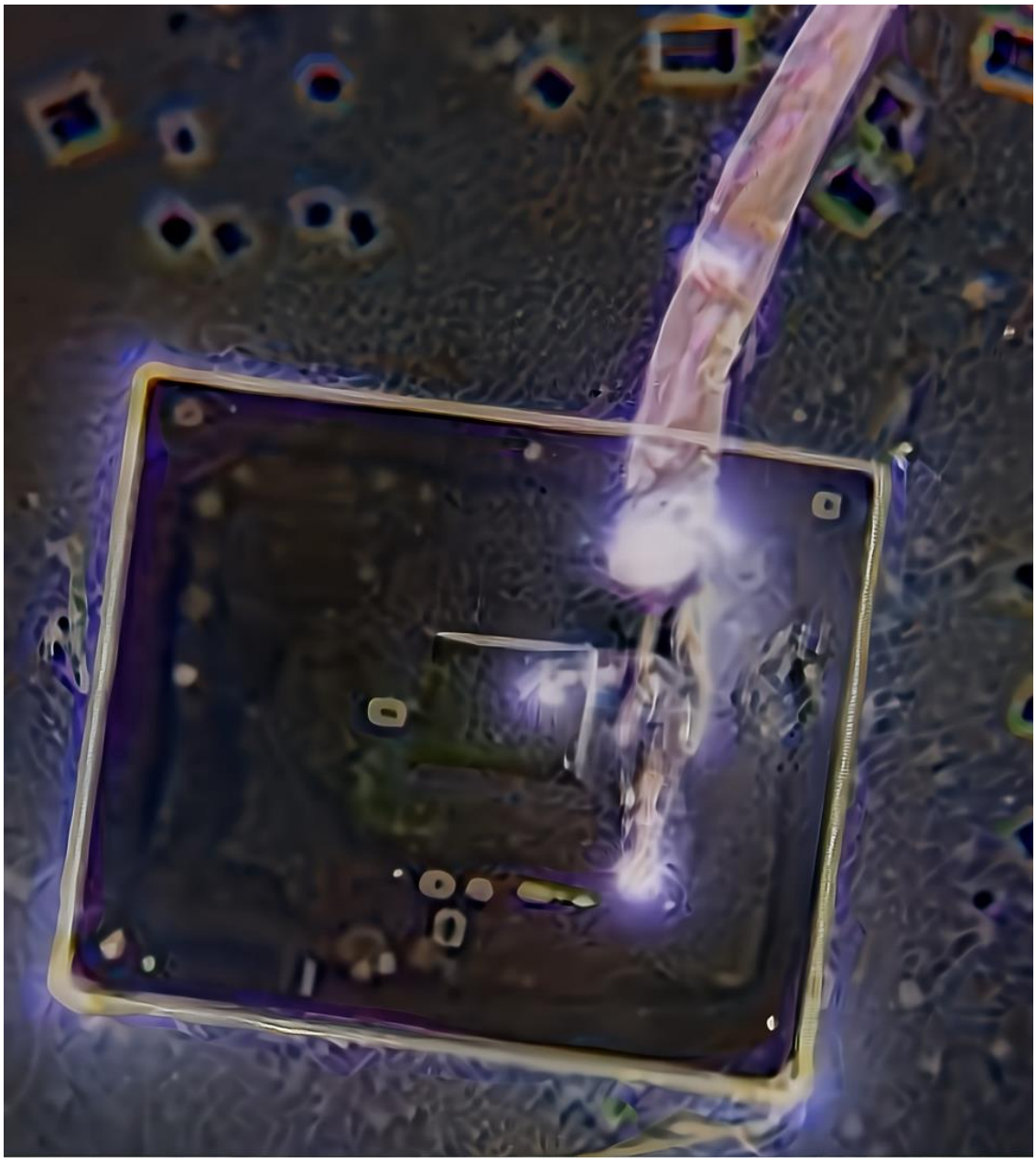

Figure 6. Inverted and contrast-enhanced image of CFA node (Pfizer-BioNTech).The square structure exhibits internal routing features, circular and oval anchoring points, and a crystalline-perimeter junction socket connected to a vertically oriented fibre. The regularity, symmetry, and internal patterning evoke parallels with microfabricated architectures. Illumination artefacts are minimal; features are consistent with observed behaviour across other CFA units and suggest latent system design and embedded function.

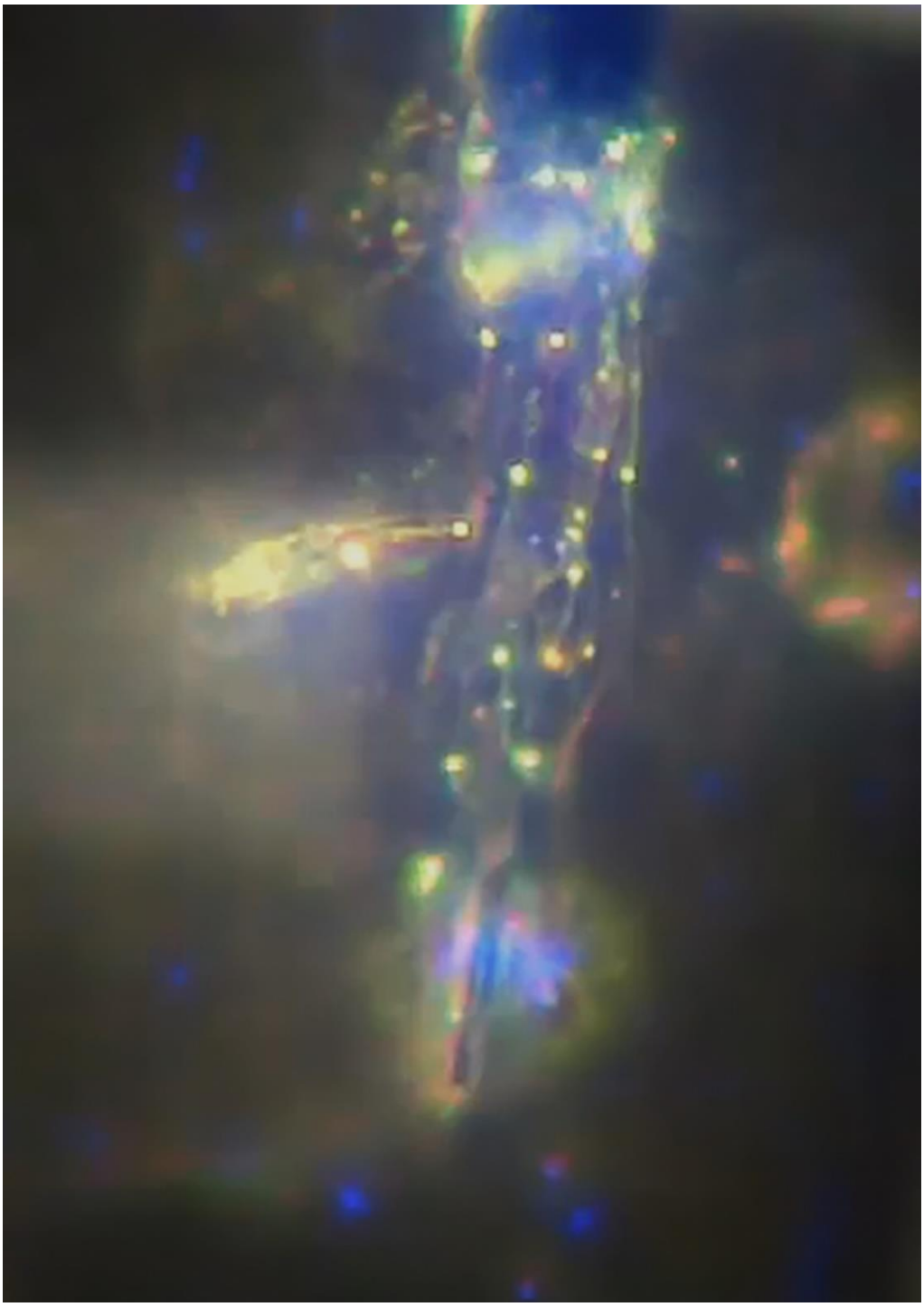

Figure 7. Enhanced dark field micrograph of a crystal–fibre junction in Pfizer–BioNTech Comirnaty. Multiple light-emitting nodes align along the central axis, suggesting coherent internal structure. The fibre appears integrated into the crystal, supporting the idea of templated or guided assembly within the CFA system. Magnification approximately 500x.

While no currently public material science literature fully accounts for the crystal–fibre interactions observed, the precision and consistency across samples suggest access to a tier of programmable microscale assembly beyond routine pharmaceutical formulation.

The possibility arises that such architectures originate from emerging or undisclosed domains of research, in which crystalline substrates and fibrous conductors operate as integrated elements within a designed system. The responsible posture, here, is not conjecture — but recognition of an unexplained order, worthy of full-spectrum investigation.

Among the pharmaceutical samples analysed, the Pfizer–BioNTech Comirnaty formulation yielded the most definitive time-resolved CFA sequence. Across a span of hours to months, crystal–fibre architectures were observed not only to persist, but to mature — exhibiting internal symmetry, node-specific light emission, and guided structural extension without external stimulus. The fibre–crystal junctions consistently revealed geometric coherence and anchoring features suggestive of programmed self-stabilisation. Collectively, this case provides the clearest evidence to date of latent architectural behaviour within an injectable formulation, supporting the classification of CFAs as Type II systems with embedded design logic and long-range organisational memory.

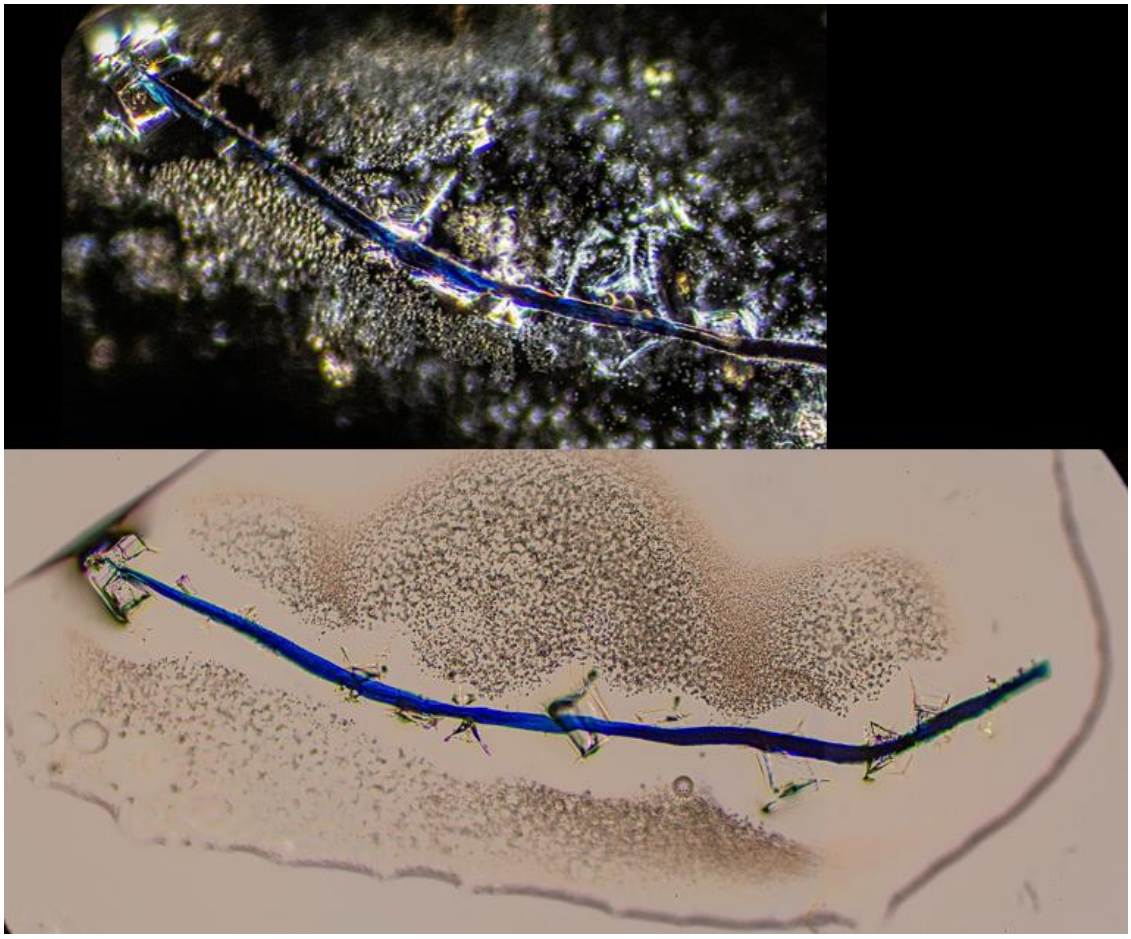

Figure 8. Paired views of a crystal–fibre assembly in a dental anaesthetic sample following sessile droplet evaporation. Dark field (top) and low-power bright field (bottom) images show the same fibre across optical regimes, demonstrating continuity, attachment of crystalline elements, and embedding within a particulate field. Magnification 200x

If the fibre in these samples were simply an inert contaminant, it would not be expected to influence how surrounding material behaves as the solvent dries. In typical drying systems, crystallisation occurs late, once most solvent has evaporated, with crystals forming irregularly at edges or pooling into disordered clusters. A passive fibre would be overgrown or buried by this process. Instead, what is observed here — and in the majority of comparable preparations examined — is earlier crystallisation distributed along the fibre, with repeated and consistent attachment rather than chaotic piling. This suggests that the fibre alters local boundary conditions during drying and participates in the organisation of surrounding material. While truly "normal" behaviour has been observed on occasion, it has been the exception rather than the rule, with most samples exhibiting some degree of fibre-associated organisation.

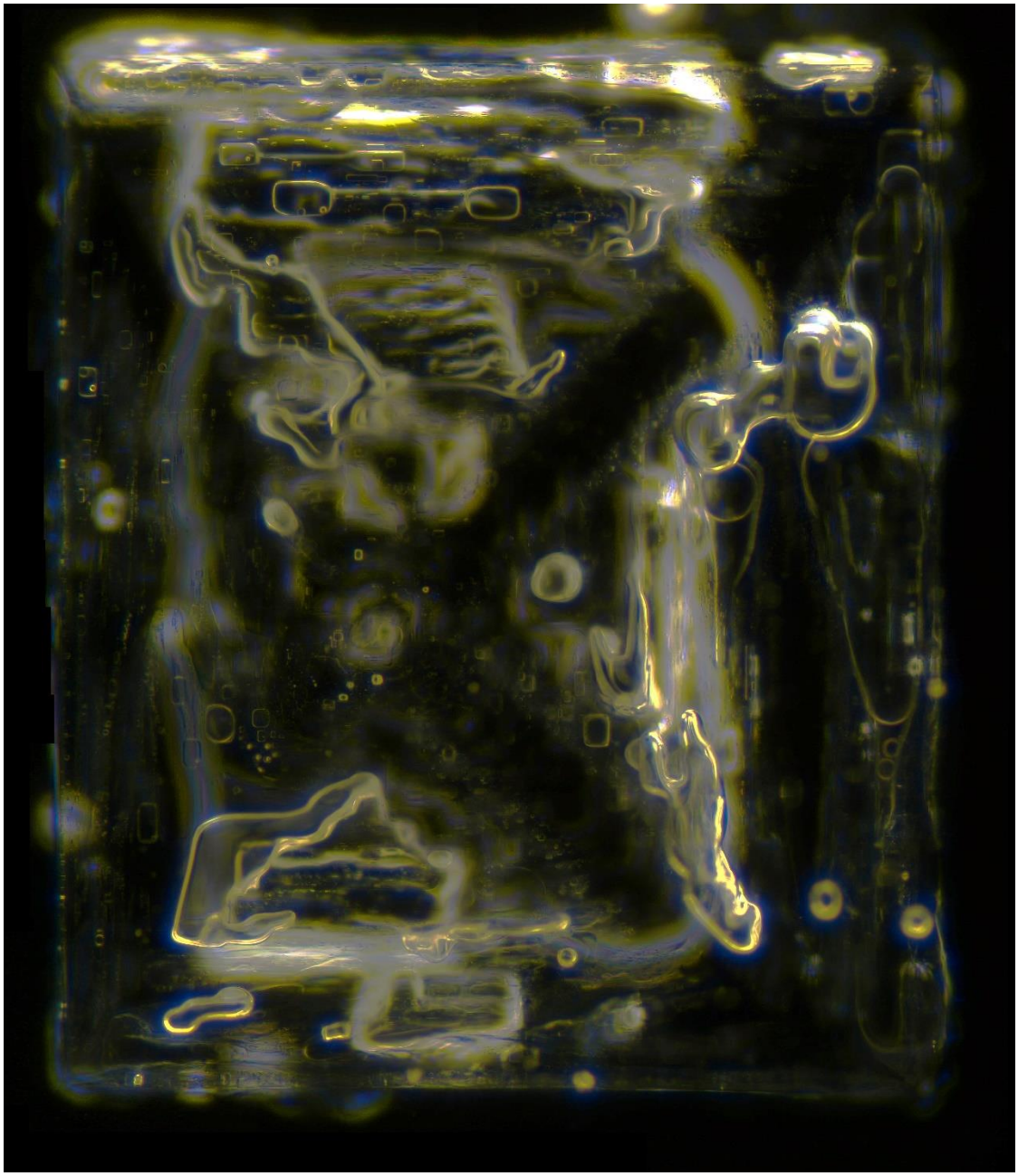

Figure 9. Complex CFA crystal formed from a dental anaesthetic following SDE (sessile droplet evaporation). The rectangular architecture exhibits layered internal organisation, including curved channels, embedded nodal points, and apparent routing lines. No external field or reagent was applied. Magnification ~40x.

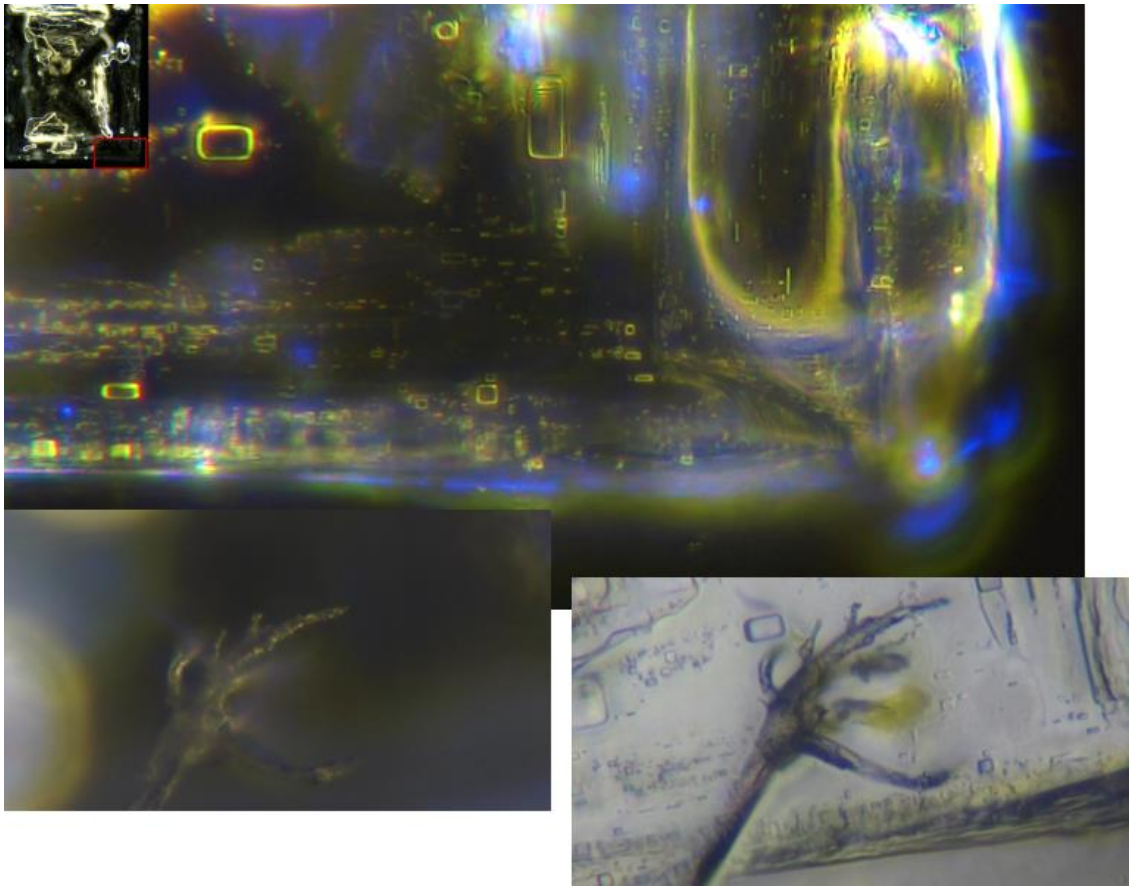

Figure 10 Composite panel showing the fibre emergence from the CFA crystal in Figure 8. Lower left: dark field image captured on day 2, revealing a branched fibre extending from the lower edge of the crystal. Lower right: bright field image of the same region, confirming fibre–crystal continuity and internal structural alignment. Inset (top left): whole-crystal overview with red box indicating region of interest.

This structure exhibited all four defining CFA criteria, including embedded crystal–fibre coupling, geometric regularity, temporal persistence, and internal nodal complexity. Initially appearing as a dense rectangular crystal, it revealed a stable, bifurcated fibre extension by day two, with continued clarity and anchoring evident over five months. The full sequence — captured across bright field, dark field, and composite imaging — represents the clearest Type II CFA in the dataset, with the fibre traversing the crystal boundary and integrating into its internal architecture. This case provides a compelling benchmark for synthetic coherence within pharmaceutical soft matter systems.

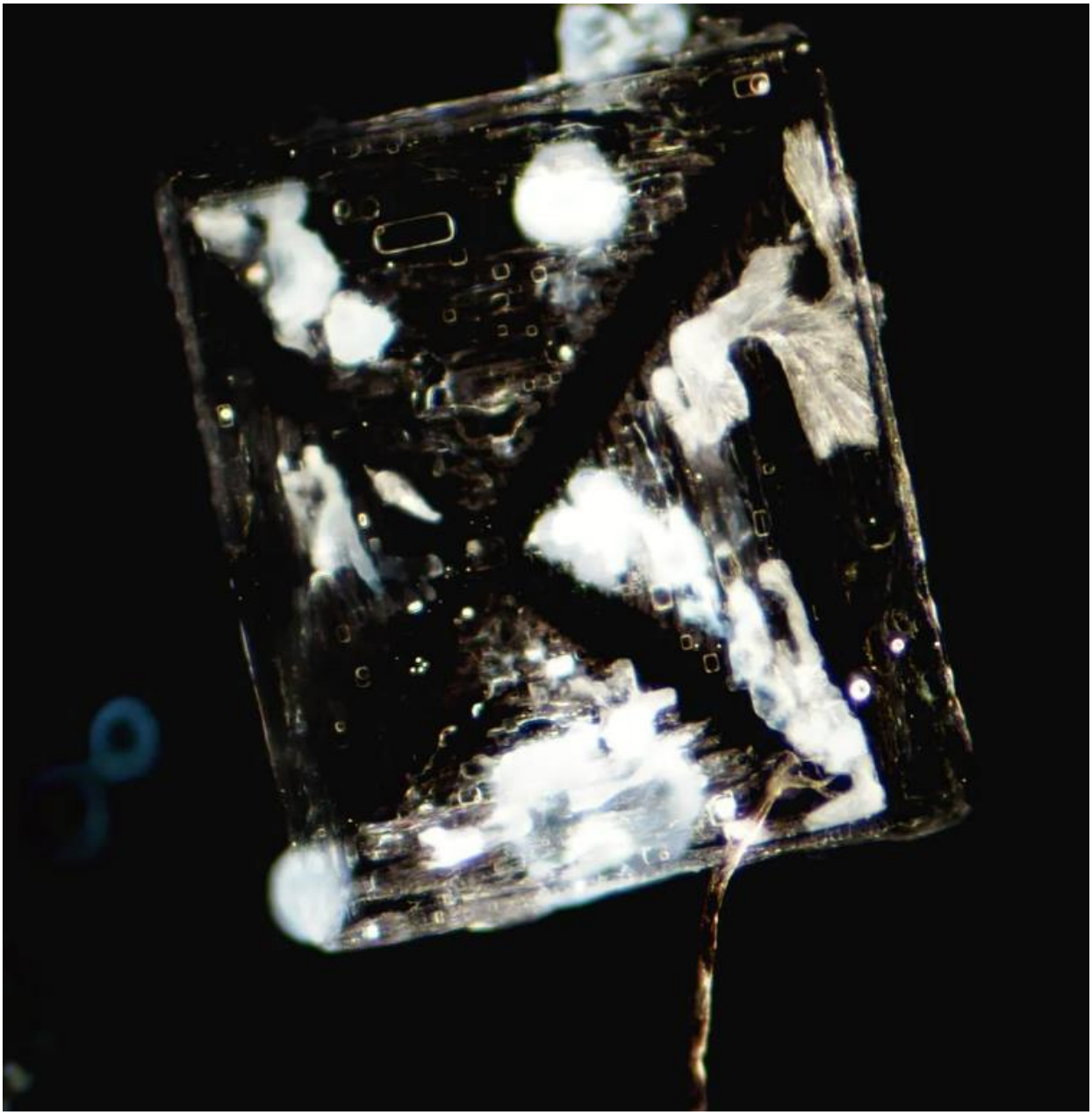

Figure 11. Dark field image of a rectilinear crystalline structure exhibiting internal Circle–Rectangle Motifs (CRMs) with an attached fibre consistent with a Crystal Fibre Assembly (CFA). The geometric organisation and fibre–crystal coupling are clearly resolved. Magnification 20x.

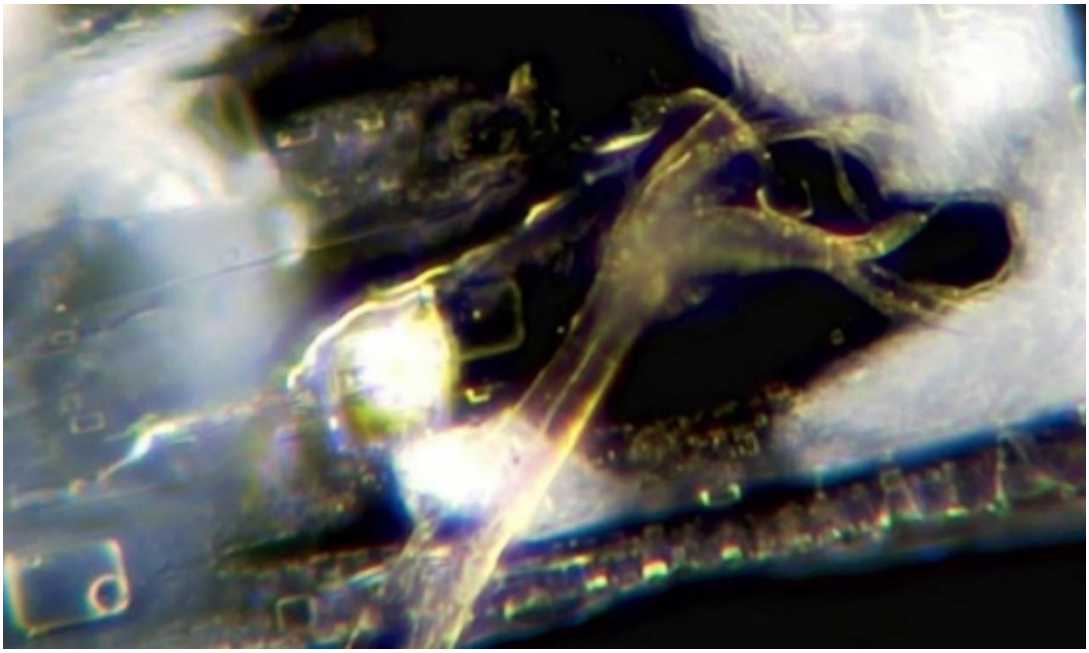

Figure 12. Dark field image of a fibre extending from a crystalline structure. Five months after initial formation, the fibre remains physically connected, indicating long-term structural stability. Magnification 200x.

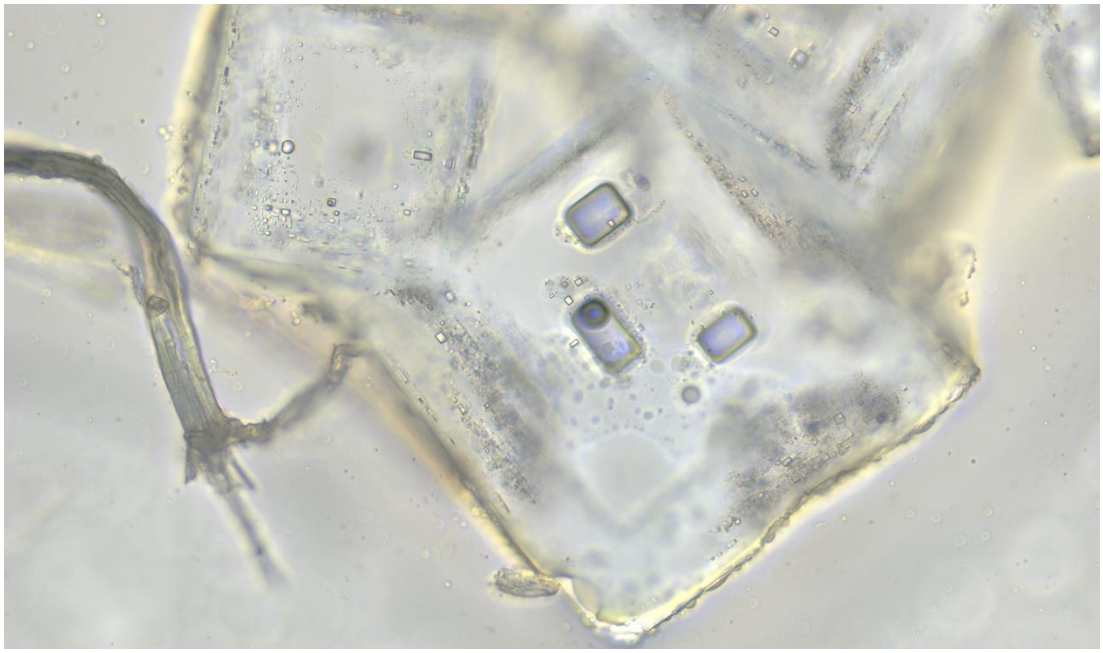

Figure 13. Dark field image of a rectilinear crystalline structure formed in a different dental anaesthetic formulation. Despite differences in surface appearance and internal clarity, the crystal exhibits the same geometric organisation and internal rectilinear inclusions observed across samples. Magnification 200x.

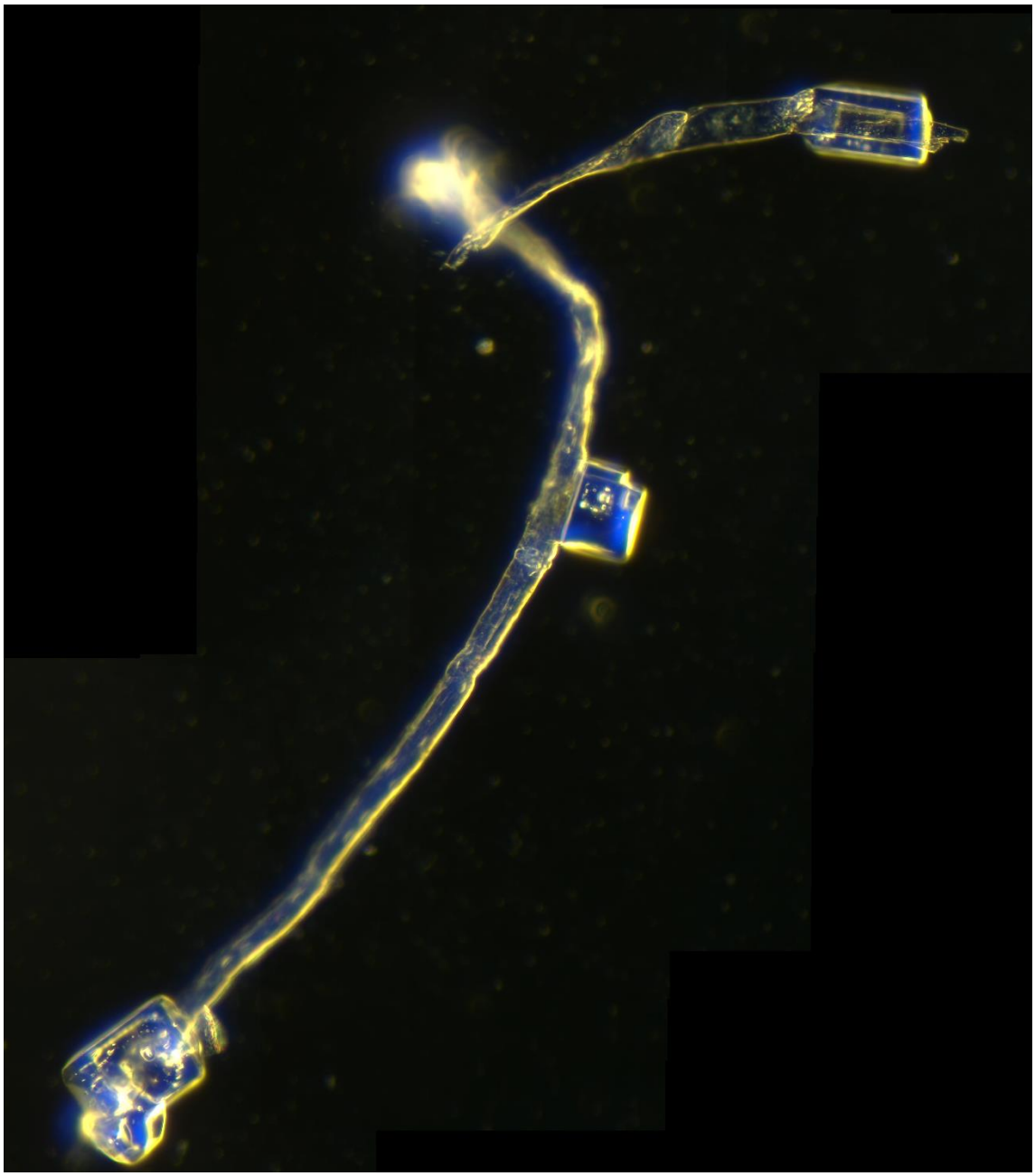

Figure 14. Crystal Fibre Assembly exhibiting functional continuity across a physically discontinuous fibre. Two fibre segments with matching optical properties, curvature, and node geometry terminate into square crystalline domains despite an intervening gap. Extended depth of field imaging captures both segments within a single frame, while non-EDF views confirm true physical discontinuity. Magnification 200x.

In several instances, fibre–crystal interactions were observed despite the absence of continuous physical contact. In the example shown in Figure X, the fibre is clearly discontinuous, with a visible gap separating two segments that nevertheless share identical optical properties, thickness, and curvature. Each segment terminates into a geometrically coherent crystalline node, and the overall configuration behaves as a single integrated assembly rather than as two independent fragments.

Extended depth of field imaging allows both fibre segments to be visualised within a single frame, while non-EDF views confirm that the discontinuity is genuine rather than an artefact of focus or motion. These observations indicate that direct material continuity is not a prerequisite for fibre-mediated influence on crystal morphology or orientation. Instead, the organisation of the system appears to be governed by non-contact interactions, suggesting that fibres may exert structural guidance or coupling effects across small spatial gaps. Similar behaviour has been documented in Pfizer Comirnaty samples, where fibres appear to maintain positional or orientational influence on crystalline domains despite apparent breaks or offsets, reinforcing the interpretation that these assemblies operate as field- or coherence-linked architectures rather than purely mechanical constructs.

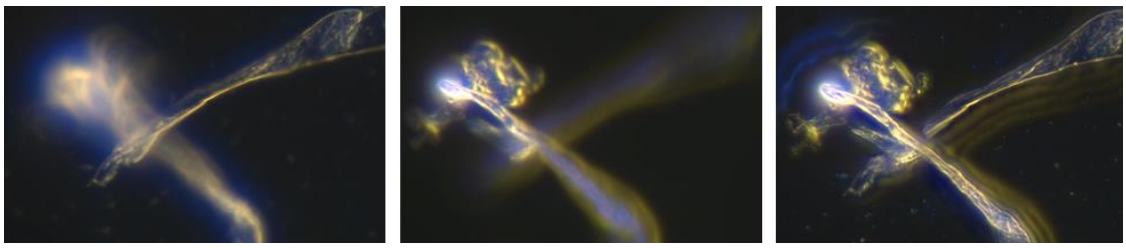

Figure 15. Sequential views of a Crystal Fibre Assembly showing functional continuity across a physically discontinuous fibre. Across panels, fibre segments with matching optical properties and curvature interact with a common crystalline node despite a visible gap. Non-EDF views confirm physical separation, while integrated imaging highlights preserved organisational coherence. Magnification 200x.

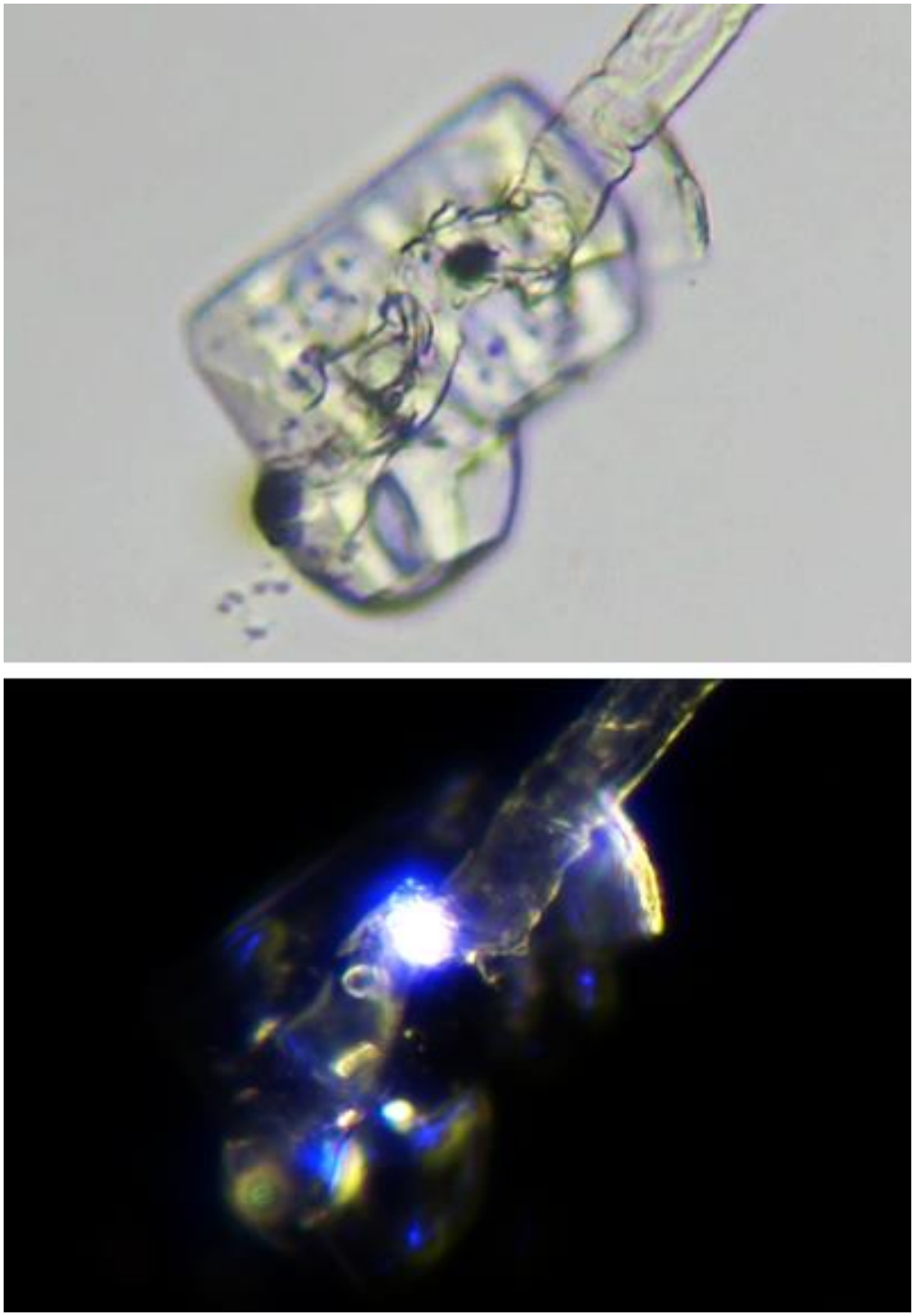

Figure 16. Paired bright field (top) and dark field (bottom) views of a Crystal Fibre Assembly node. Bright field imaging reveals the physical geometry of the crystal–fibre junction, while dark field imaging highlights concentrated optical activity at the crystalline domain and along the associated fibre. Magnification 200x.

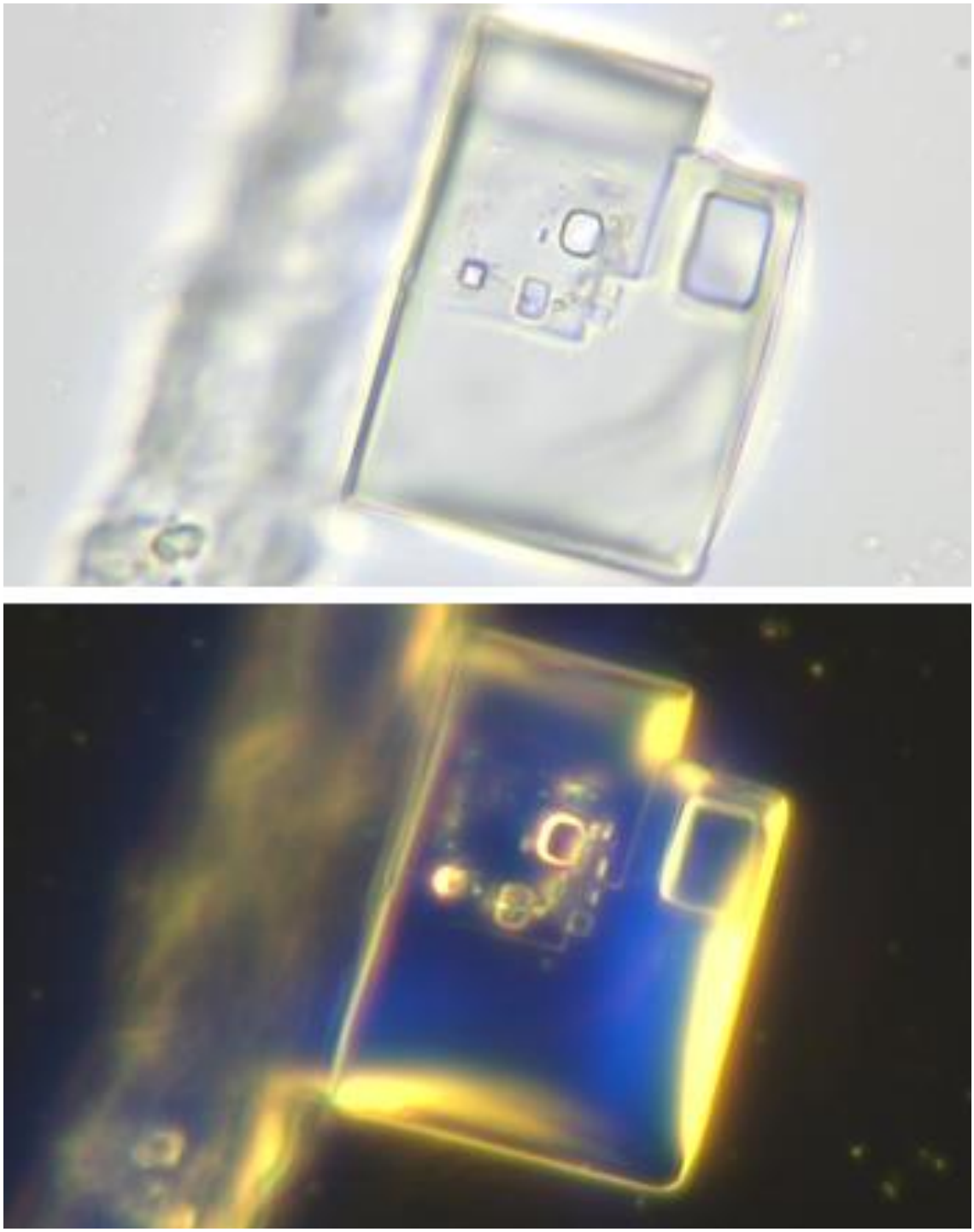

Figure 17. Paired bright field (top) and dark field (bottom) views of a square crystalline domain with internal rectangular inclusions. Bright field imaging reveals well-defined external geometry and internal features, while dark field imaging highlights pronounced optical activity concentrated at crystal edges and internal domains. Magnification 200x.

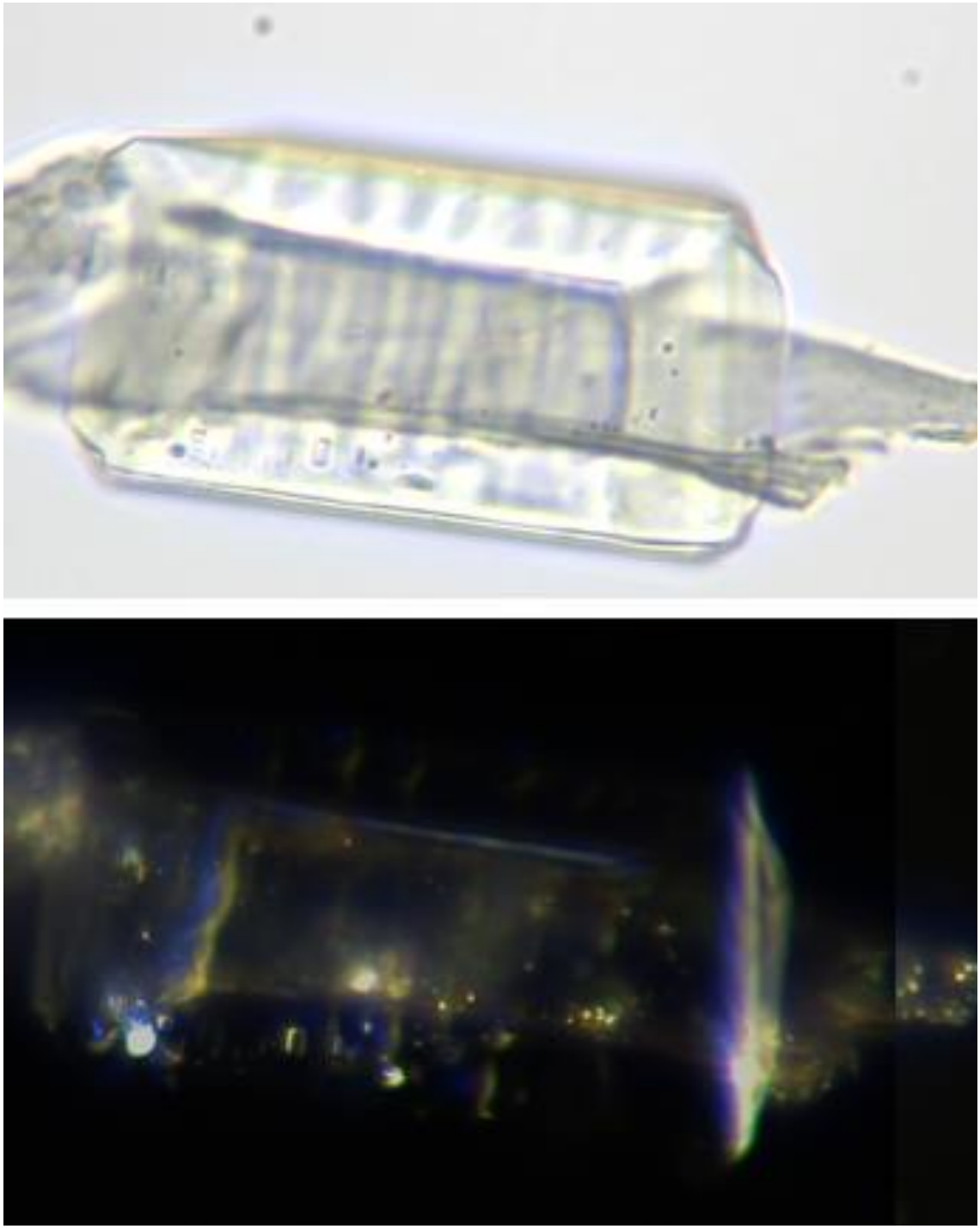

Figure 18. Paired bright field (top) and dark field (bottom) views of an elongated crystalline structure with internal longitudinal banding. Bright field imaging reveals parallel internal features and defined external geometry, while dark field imaging highlights optical activity distributed along the crystal length and internal domains. Magnification 200x.

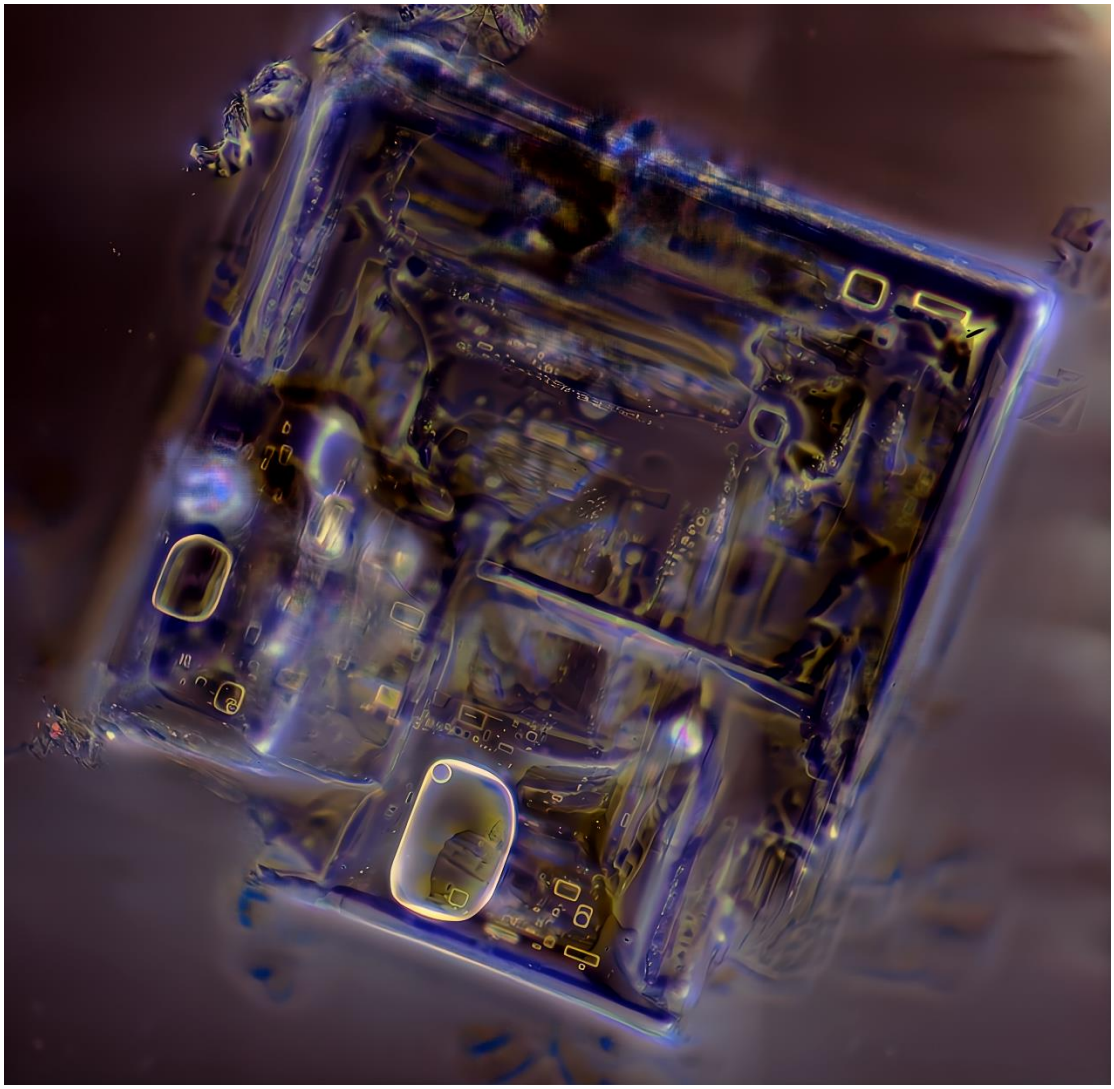

Figure 19. Inverted bright field image of a CFA-like assembly formed after a second sessile droplet evaporation (SDE) cycle in plain generic lignocaine (manufactured in India). The structure exhibits highly ordered rectilinear compartments, nodal enclosures, and repeating motifs suggestive of templated growth. Assembly occurred without external fields or additives, reinforcing the phase-dependent emergence of crystalline–architectural forms under ambient conditions. Magnification ~400x.

Notably, small-scale CFA-like structures were also observed in non-dental local anaesthetic preparations, including compact junctional forms exhibiting localised optical activity (Figure 18, mid-left), indicating that CFA formation is not restricted to a single formulation or clinical context.

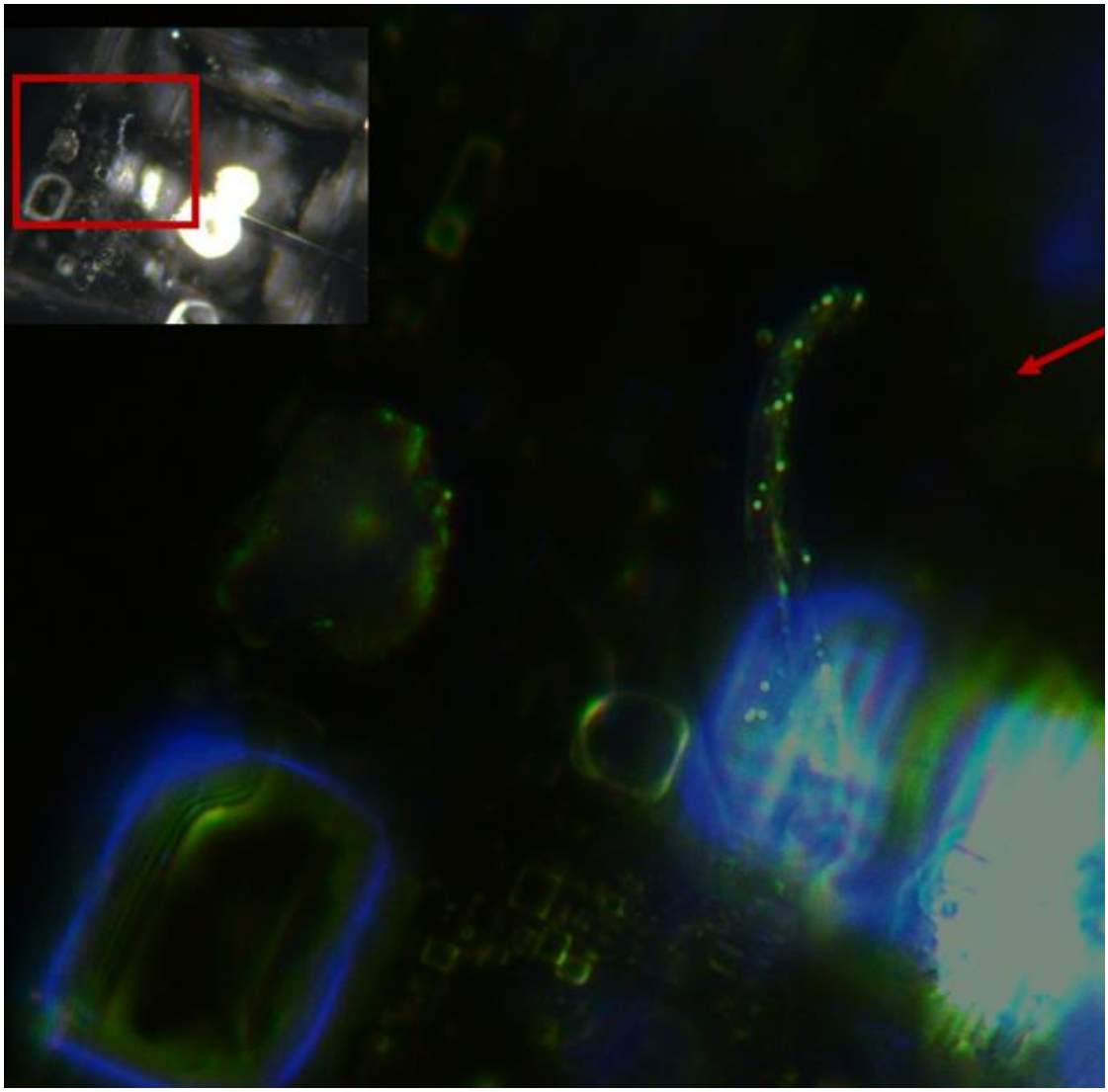

Figure 20. Close-up dark field image of the CFA junction on the same lignocaine crystal shown in Figure 12. The fibre emerges from a defined edge socket and exhibits nodal highlights along its arc, consistent with previous CFA architectures. Inset (top left) shows the broader crystal context with the region of interest highlighted. Magnification ~500x.

Comparable fibre–crystal integration was also observed in Moderna mRNA vaccine samples, where fibrous elements were embedded within crystalline domains at the micrometre scale (see Figure 20).

Figure 21. Fibre integrated within a crystalline structure in a Moderna mRNA vaccine sample. Dark field microscopy reveals a fibrous element embedded within and traversing a multi-lobed crystalline assembly, with apparent mutual constraint between fibre curvature and crystal morphology.

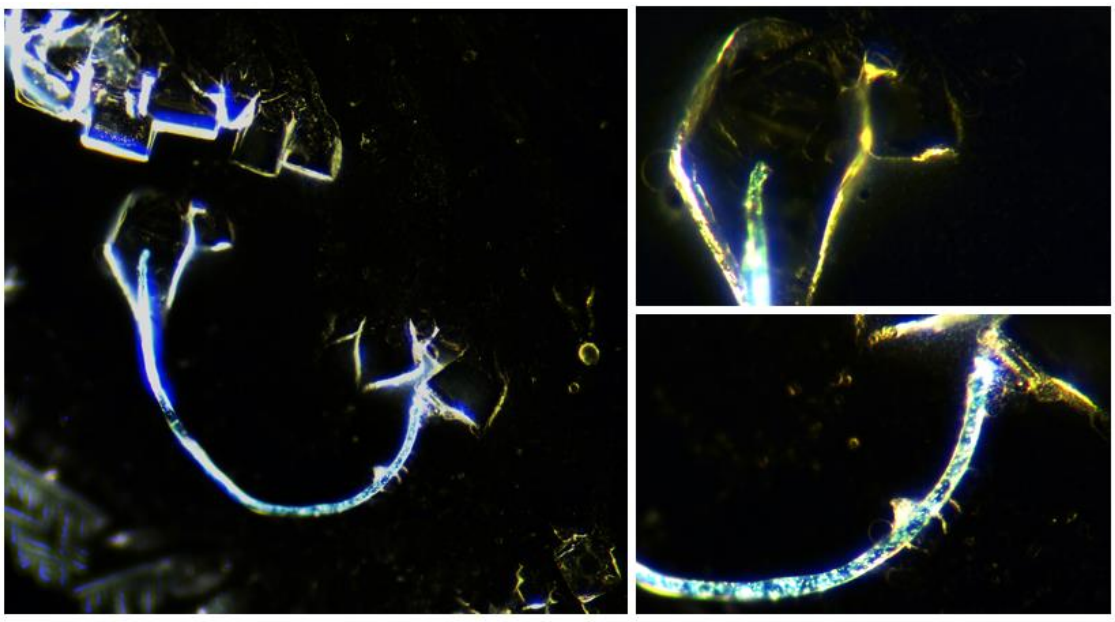

Figure 22. Multi-panel presentation of a Crystal Fibre Assembly (CFA) formed in an influenza vaccine following four successive Sessile Droplet Evaporation (SDE) cycles. Left: overview showing a continuous curved fibre linking multiple angular crystalline domains in a closed-loop architecture. Right (top and bottom): higher-magnification views of CFA junctions and fibre segments, revealing defined attachment sites, internal particulate inclusions, and sustained optical activity along the fibre length. Magnification 400x.

The following image is notable for the clarity of the fibre–crystal relationship. Unlike examples where fibres appear attached to, aligned with, or adjacent to crystal surfaces, the fibre here directly penetrates the crystalline domain and persists internally, maintaining continuity across the crystal boundary. The crystal itself remains well defined, with no evidence of fracture, dissolution, or boundary distortion at the point of entry.

This suggests that direct physical contact between fibres and crystal surfaces is not a prerequisite for structural influence, and that fibres may act as internal organising elements or templates during crystallisation. The observation is particularly significant given the simplicity of the system: budesonide is chemically and formulation-wise distinct from vaccines and dental anaesthetics yet exhibits the same architectural motif. This supports the interpretation that Crystal Fibre Assemblies represent a generalisable self-assembly behaviour under certain conditions, rather than a formulation-specific anomaly.

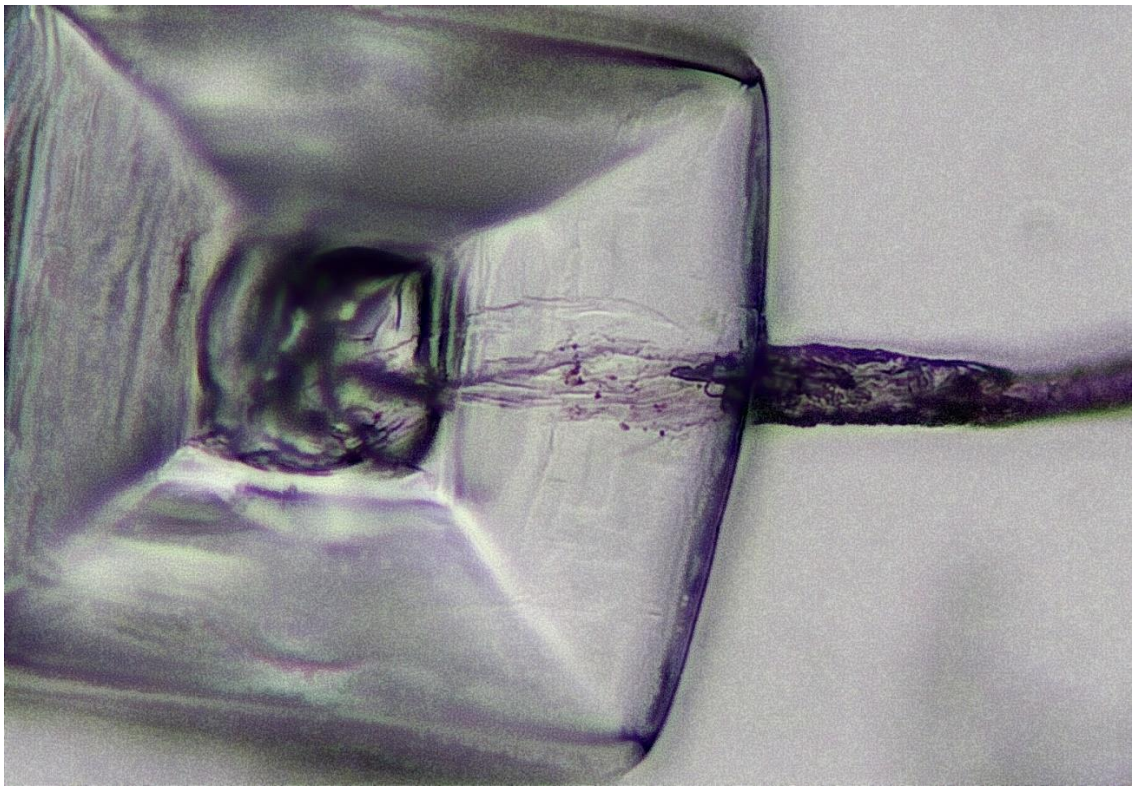

Figure 23. Crystal Fibre Assembly observed in a budesonide preparation following sessile droplet evaporation. A linear fibre traverses the crystalline domain, entering through one face and continuing internally without apparent disruption to crystal geometry. Bright field imaging. Magnification 200x.

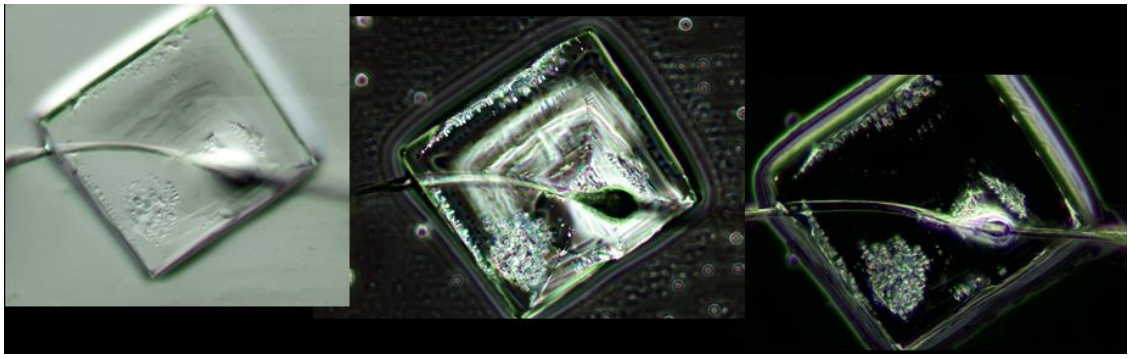

Figure 24. Bright field, phase contrast, and dark field views of a budesonide Crystal Fibre Assembly showing a continuous fibre traversing the crystalline domain, with modality-dependent emphasis of geometry, internal structure, and optical activity. Magnification 200x.

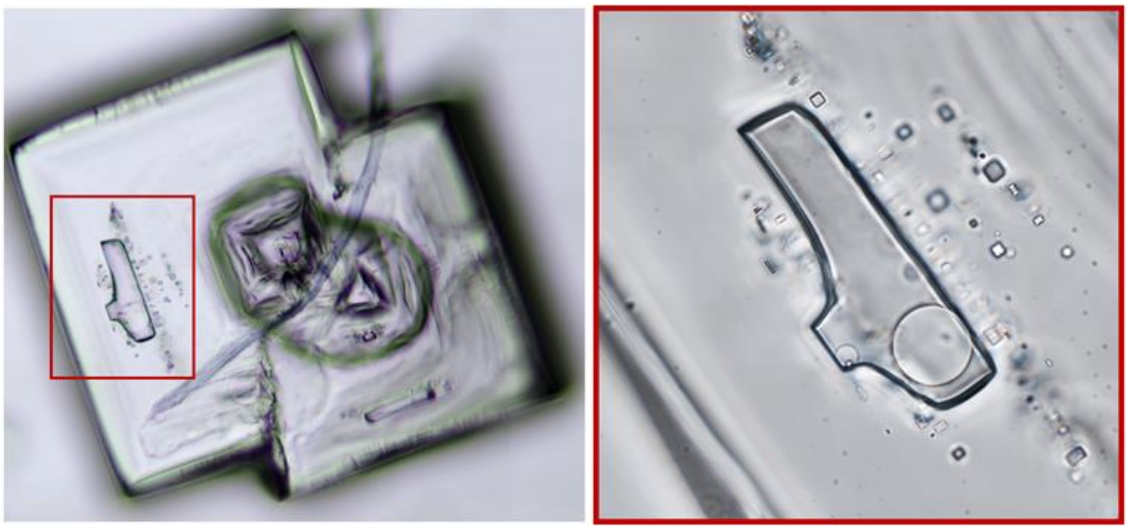

Figure 25. Bright field view of a budesonide crystalline domain containing an internal elongated microform (boxed), shown at higher magnification on the right. The inclusion exhibits sharp rectilinear boundaries, a stepped geometry, and a rounded terminal feature, distinct from surrounding crystalline texture. Magnification 200x (left), approx. 600x (right).

This structure differs from previously documented Crystal Fibre Assemblies in that the internal element is fully enclosed within the crystalline domain rather than acting as an external or traversing fibre. The elongated, tool-like geometry and sharply defined edges indicate organised internal structuring rather than incidental particulate inclusion. Its consistent morphology across magnification levels, combined with the absence of disruption to the surrounding crystal lattice, suggests a templated or phase-coupled formation process occurring during crystallisation.

The presence of such internally bounded forms in budesonide extends the CFA framework beyond surface-associated fibres, indicating that structured architectures may also emerge as enclosed, spatially constrained elements within pharmaceutical crystals.

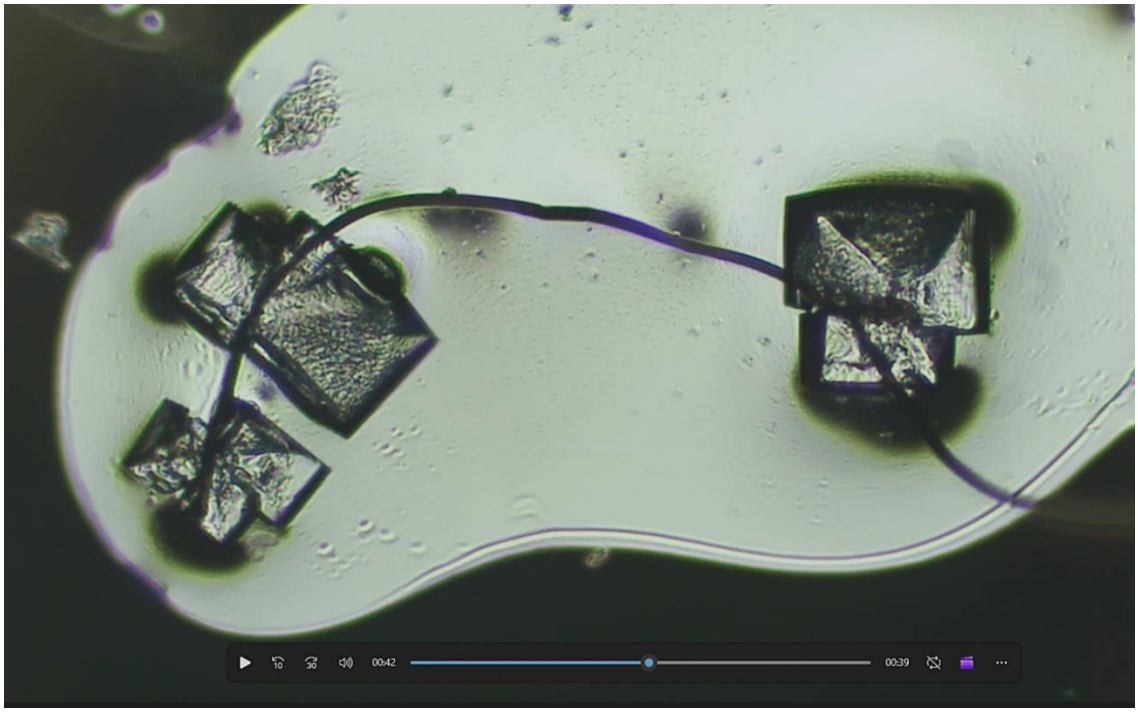

Figure 26. Time-lapse video still showing three discrete crystalline domains forming sequentially along a single continuous fibre during sessile droplet evaporation. The fibre remains structurally intact while serving as a shared nucleation scaffold for multiple crystals. Magnification 200x.

This sequence does not conform to classical homogeneous nucleation, in which crystals form independently within the bulk solution or pool chaotically at late stages of drying. Instead, time-resolved imaging shows multiple crystalline domains emerging sequentially at distinct sites along a pre-existing fibre. The persistence of the fibre throughout the process, combined with the ordered spatial and temporal pattern of nucleation, indicates heterogeneous, fibre-guided crystallisation.

Such behaviour is consistent with non-classical crystallisation pathways and supports the interpretation of fibres as active structural participants in Crystal Fibre Assembly formation rather than passive byproducts of crystallisation.

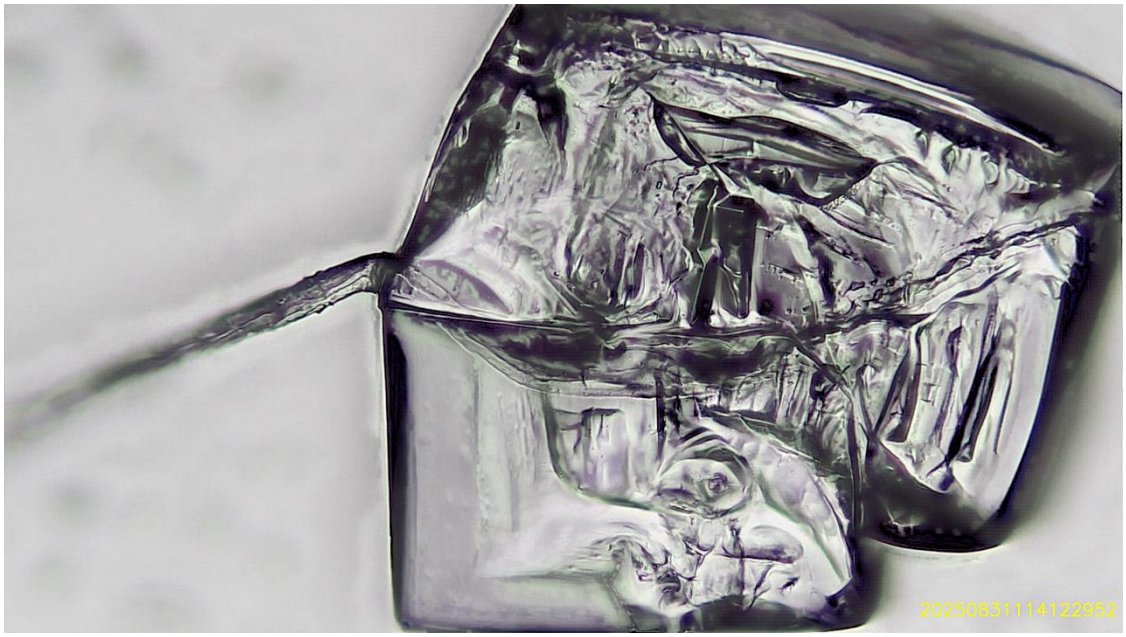

Figure 27. Budesonide crystal intersected by a continuous fibre, with the crystalline body spanning and incorporating the fibre rather than terminating at it. Internal striations and edge distortions are visible at the fibre–crystal interface. Magnification 400x.

In this configuration, the crystal does not nucleate adjacent to the fibre but instead incorporates it within the crystalline body, indicating that the fibre was present during crystal growth rather than attaching after maturation. The uninterrupted continuity of the fibre across the crystal interior, together with internal texturing aligned to the fibre axis, is inconsistent with incidental post hoc contact. Instead, the arrangement supports a coupled formation process in which fibre and crystal emerged within a shared phase domain under altered boundary conditions at the blood–air interface.

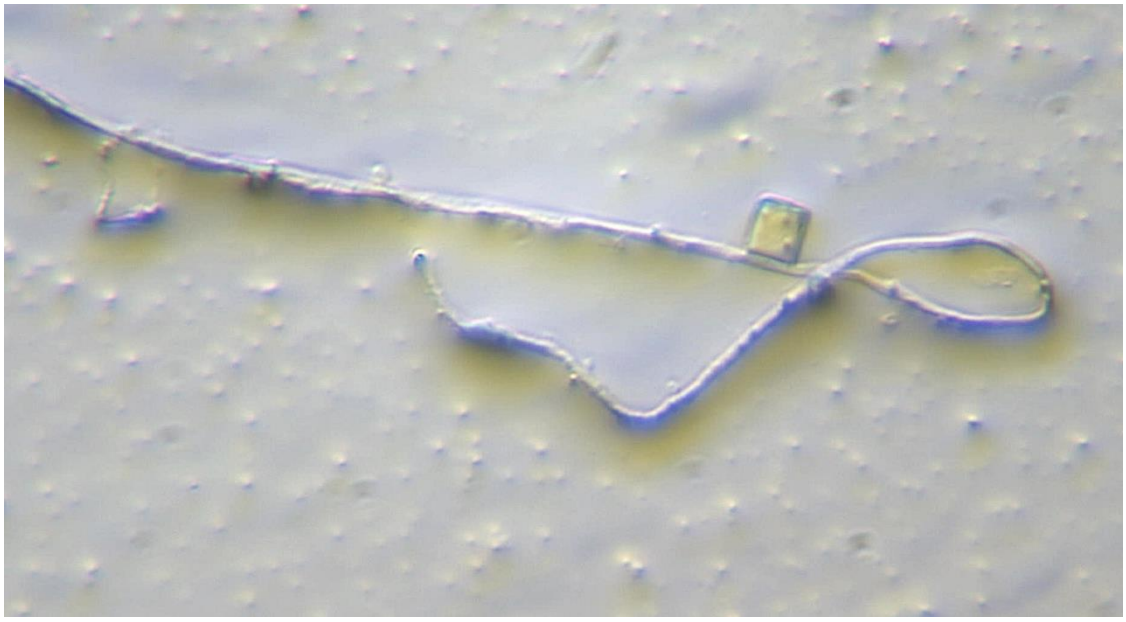

Figure 28. Continuous fibre with a single square crystal anchored along its length at the edge of a blood sample following prolonged magnetic proximity. The fibre traverses the crystal without interruption and forms a distal loop beyond it. The sample was maintained in proximity to a magnet for approximately 12 hours prior to imaging. Magnification 400x.

This image was obtained at the peripheral zone of a blood sample after approximately 12 hours of proximity to a static magnet. A single square crystal is observed anchored directly to a continuous fibre, which traverses the crystal boundary without interruption and extends into a distal loop.

The preservation of fibre continuity at the crystal interface, together with the prolonged exposure to a magnetic field, suggests that this configuration did not arise from incidental post hoc contact. Instead, the geometry is consistent with phase-coupled organisation within a field-influenced environment, where fibre and crystal appear to have stabilised as part of a shared structural domain at the blood–air interface.

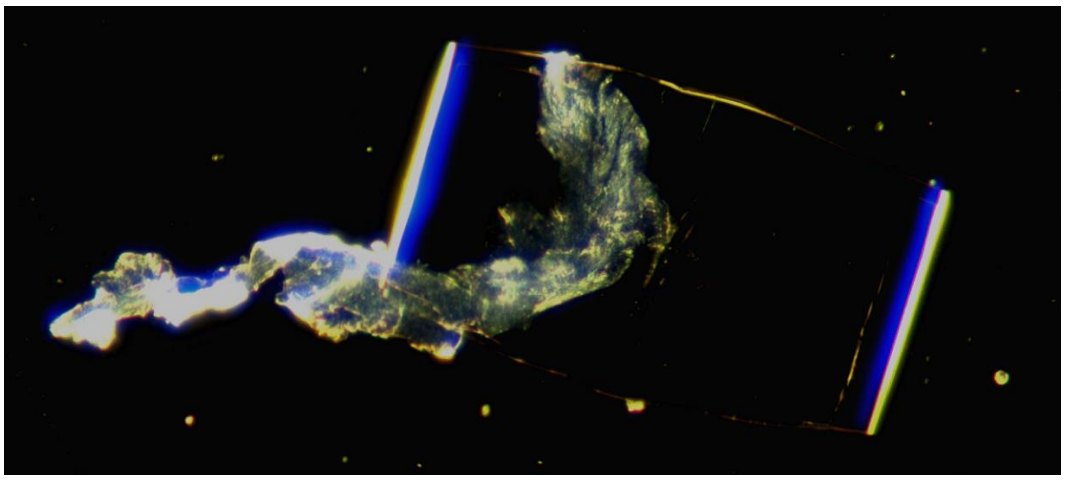

Figure 29. Dark field image of a fibre-associated crystalline structure observed in a urine sample. The fibrous element shows apparent coupling to a crystalline domain with localised optical activity. This was a rare finding and the only CFA-like structure identified in urine samples analysed in this study. Magnification 200x.

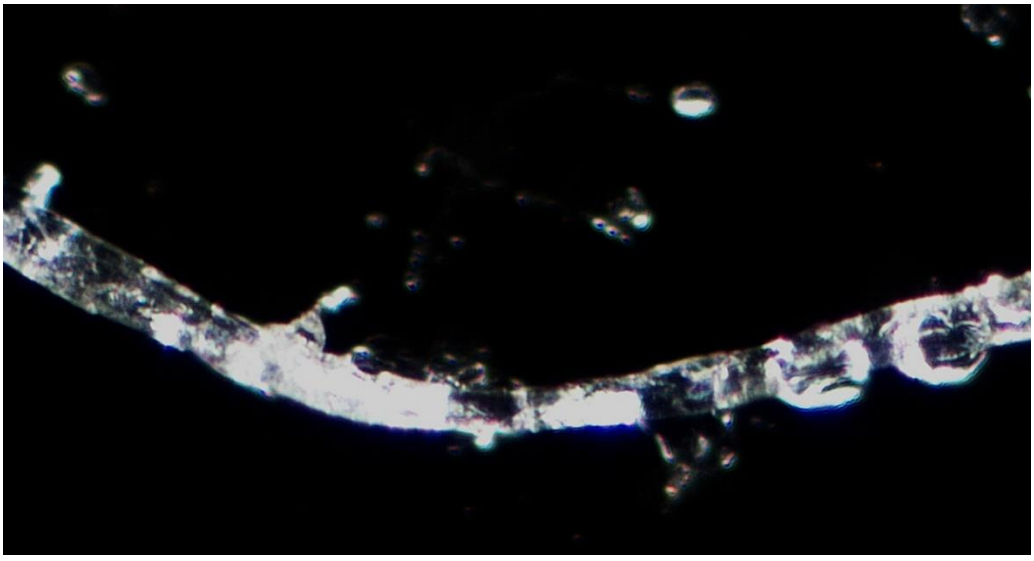

Figure 30. Continuous filament observed in an infant saliva sample. The structure exhibits non-uniform internal texture and discrete attached microdomains along its length, with optical continuity maintained across the field. Surrounding particulate material is sparse relative to the filament itself. Dark field microscopy. Magnification 100x.

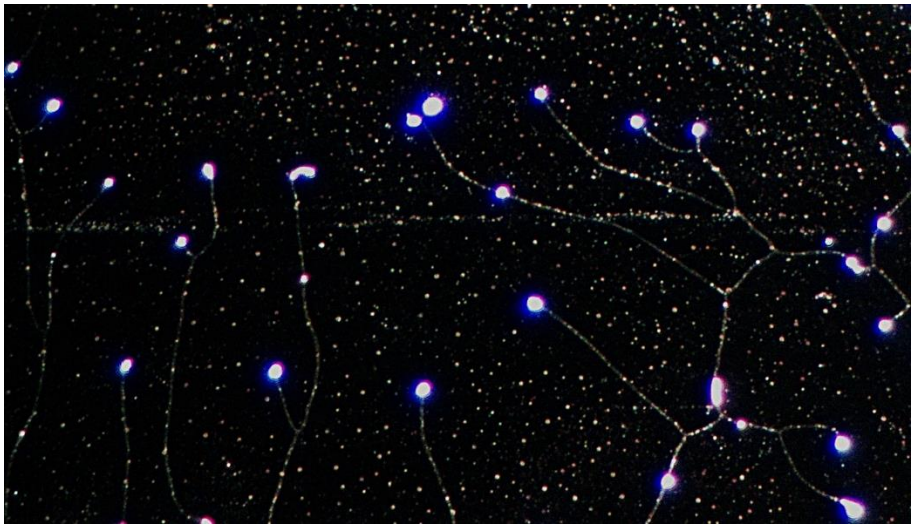

Figure 31. Fibre-associated network observed in a nasal secretion sample. Numerous fine filaments form an interconnected, branching structure with repeated bright nodal domains distributed along fibre lengths. The surrounding field contains diffuse particulate material, while the filament network exhibits continuity and coordinated geometry across the field. Dark field microscopy. Magnification 100x.

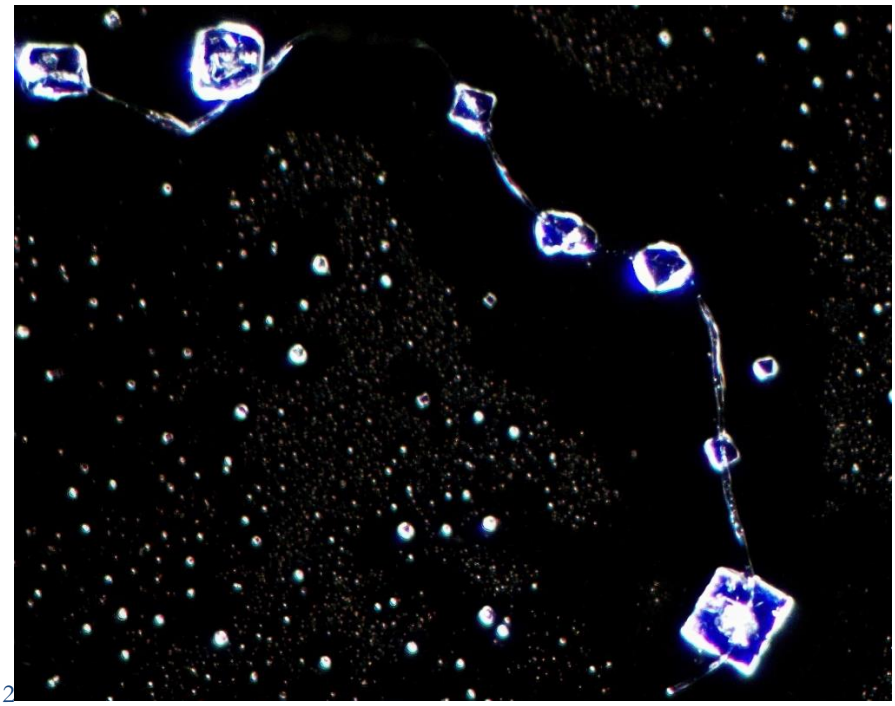

Figure 31. Crystal–fibre assembly observed in a rural water sample stored in a copper vessel. Multiple square and rectangular crystalline domains are aligned along a single continuous fibre, maintaining consistent orientation and spacing across the field. Magnification 400x.

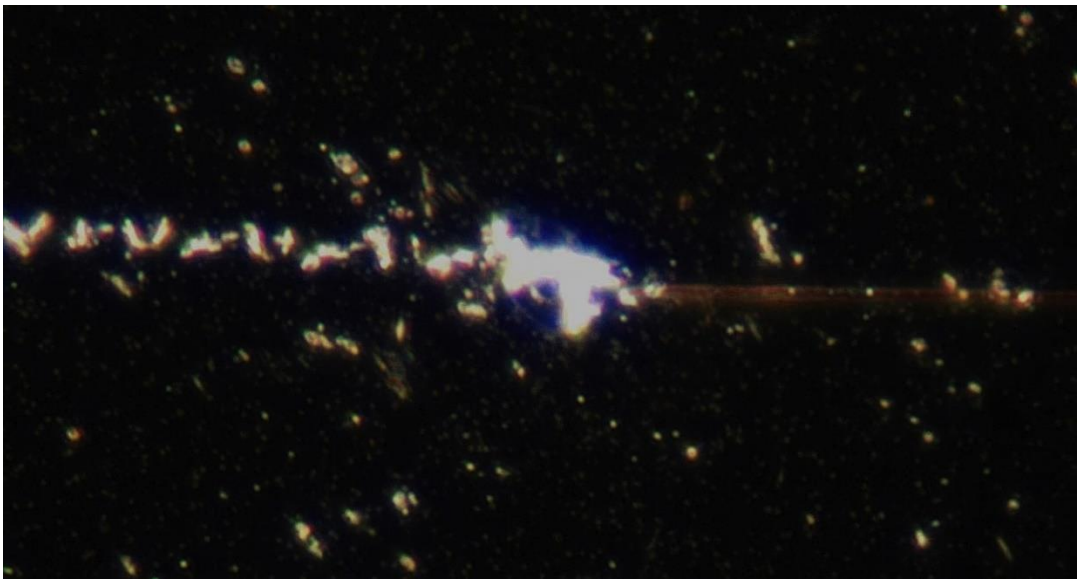

Figure 33. Field-associated phase transition in a humic/fulvic acid solution. Following approximately two hours of proximity to a static magnetic field, dispersed colloidal material exhibits axial alignment, converging into a localised phase transition marked by the emergence of a continuous fibre. Dark field microscopy. Magnification 400x.

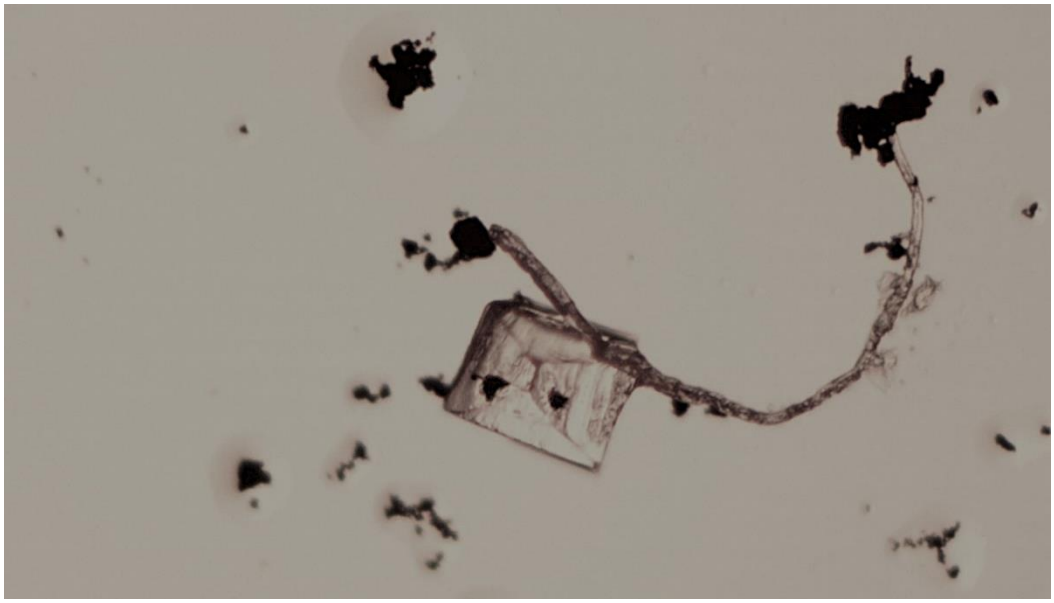

Figure 34. Activated charcoal in water showing a fibre-associated rectangular crystalline inclusion with surrounding dark aggregates. The background field contains diffuse particulate halos and irregular microdomains consistent with adsorbed material rather than free crystalline growth. Magnification 400x.

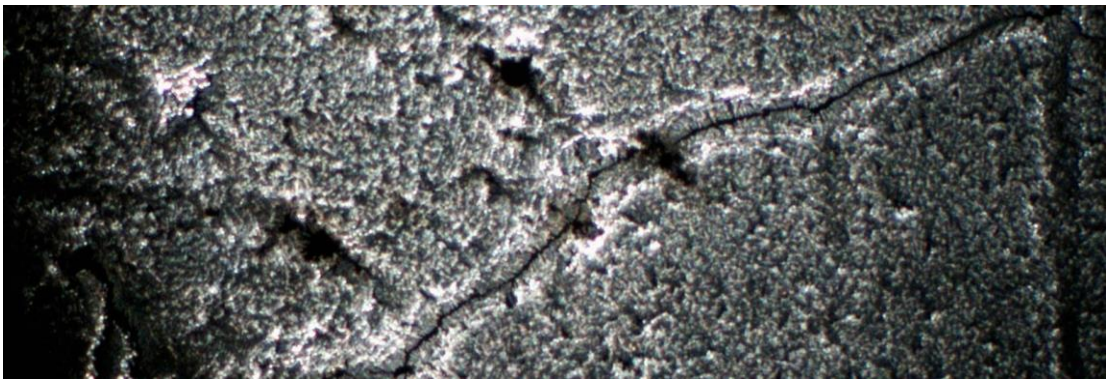

Figure 35. Dark-field image of a commercially manufactured saline solution showing diffuse particulate sedimentation with faint linear boundary traces. No fibre-associated or CFA-like structures are present. Magnification 400x.

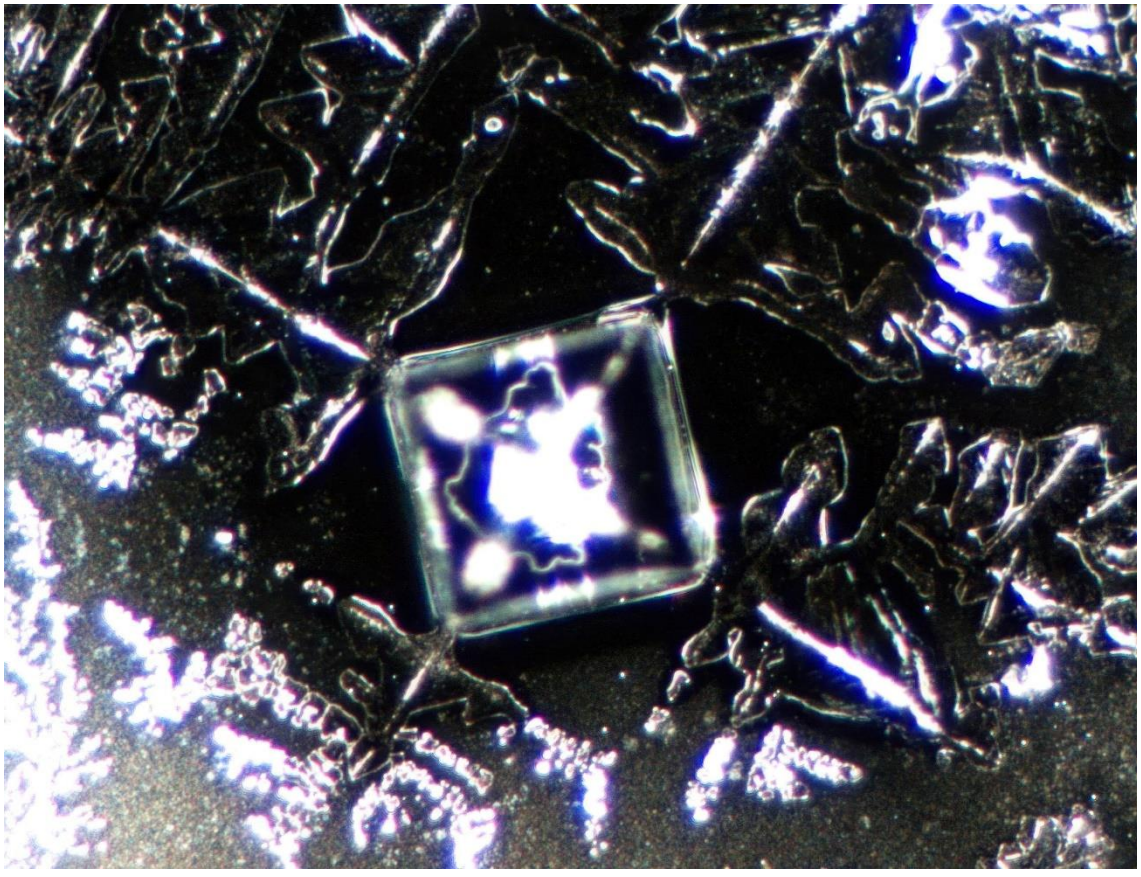

Figure 36. Dark-field image of a geometrically regular, square crystalline domain embedded within a filament-rich, sedimented matrix. The crystal exhibits sharp faceting and internal optical regularity. Surrounding elongated filamentary elements show directional coherence and appear to intersect or terminate at the crystal boundary, though no single continuous fibre traverses the field. Magnification 400x.

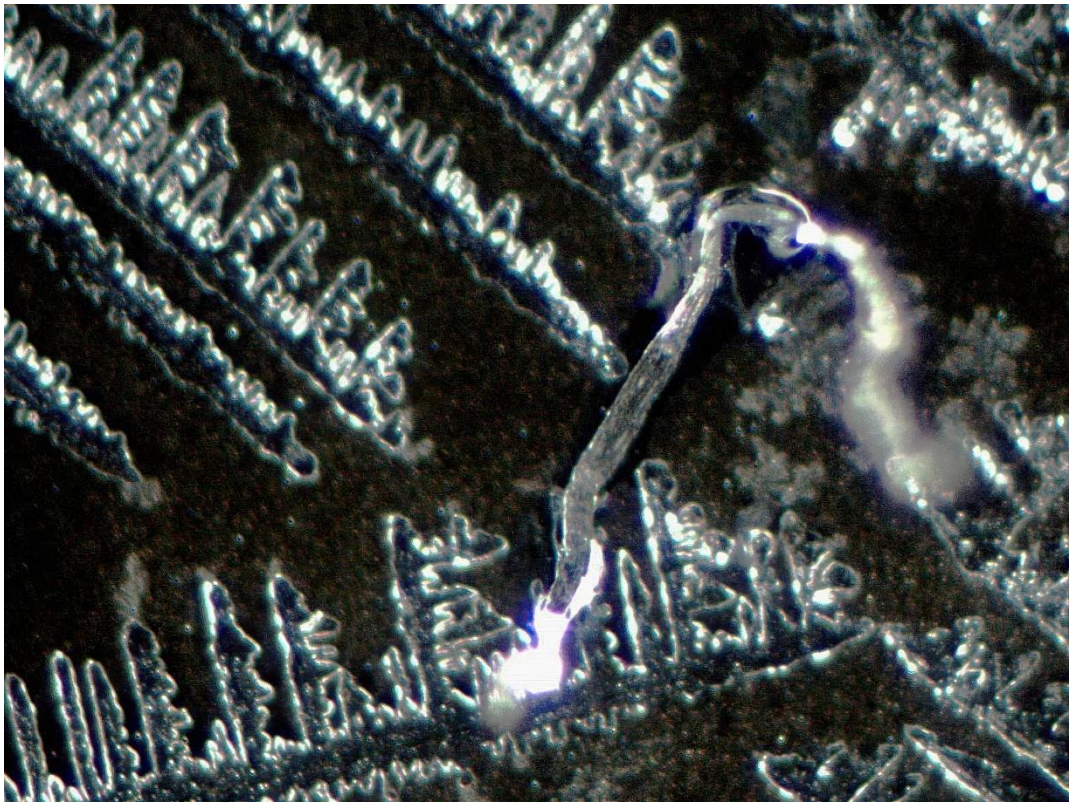

Figure 37. Dark-field image showing a fibre emerging from and traversing a dark, regular crystalline domain, set against a background of diffuse sedimentation. The fibre maintains optical continuity across the crystalline interface. Magnification 400x.

Taken together, these images delineate the minimal conditions under which crystal–fibre assemblies are observed. Commercially manufactured saline alone exhibits diffuse particulate sedimentation with faint linear boundary traces, but no fibre-associated or CFA-like organisation. When saline is combined with tears and epithelial cells, the field becomes strongly templated, producing visually striking crystalline and particulate patterning; however, this organisation remains discontinuous and lacks a continuous filamentary phase.

In contrast, the CFA-positive image demonstrates a continuous fibre emerging from and traversing a dark, geometrically regular crystalline domain, maintaining optical continuity across the crystal interface despite a sedimented background. The filamentary phase present in this case is absent from saline-only and saline–epithelial preparations under comparable conditions. These observations indicate that while ionic carrier environments and biological material can generate templated or crystalline structure, CFA formation requires the presence of a continuous filamentary component capable of coupling to crystalline domains, rather than crystallisation or templating alone.

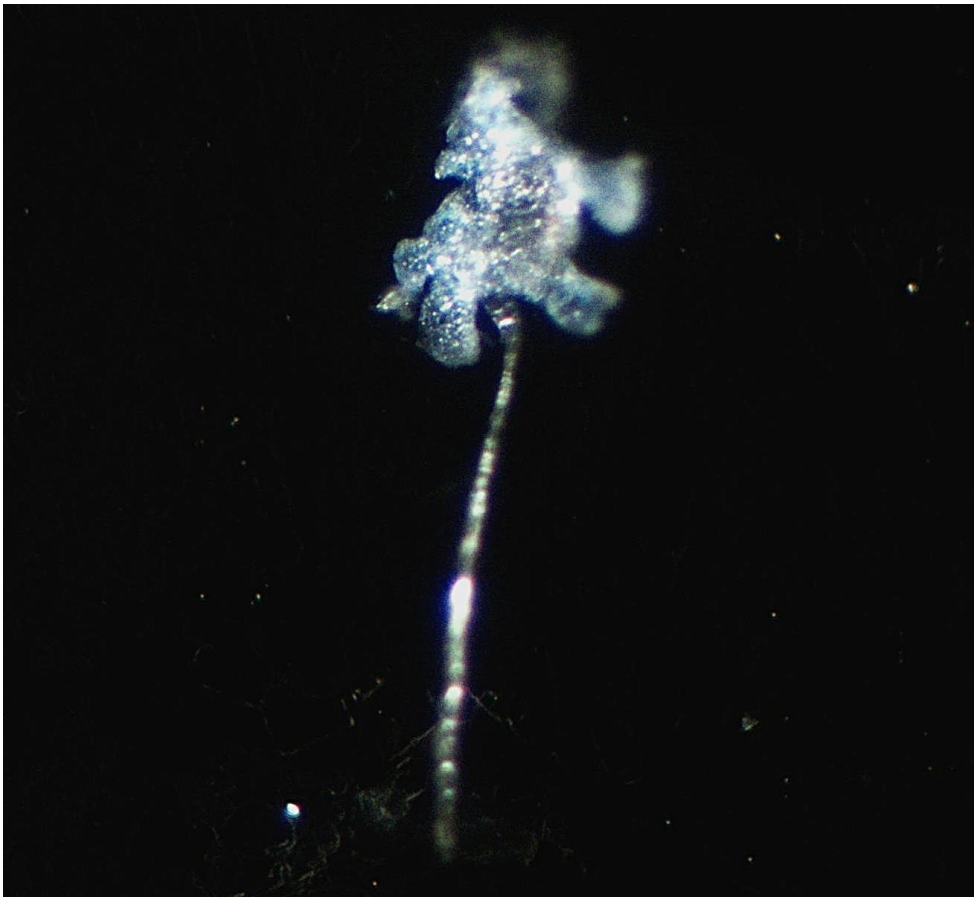

Figure 38. Dark-field image of an epithelial cell cluster exhibiting blue-shifted particulate scattering, with a coherent filament projecting from the aggregate into the surrounding field. The filament maintains optical continuity and punctate luminance along its axis, distinct from background scatter. Image adjusted only using basic exposure and contrast controls. Magnification 400x.

Figure 38 completes the minimal-condition sequence by demonstrating a continuous filamentary structure directly associated with an epithelial cell cluster, in the absence of an extended crystalline scaffold. The fibre projects from the cellular aggregate with maintained optical continuity and discrete internal texture, distinct from background particulate scatter. When considered alongside Figures 35-36, this image establishes that while crystalline domains can template organisation, they are not required for filament initiation.

Instead, the defining requirement for crystal–fibre assembly is the presence of a continuous filamentary phase capable of coupling to, traversing, or independently organising within structured environments. This observation confirms that CFA formation is not reducible to crystallisation, drying artefact, or surface templating alone, but reflects an emergent filament-driven process that can originate within biological material and subsequently interface with crystalline domains when present.

Bovine semen samples exhibit dense phase separated aggregates, angular inclusions, and continuous filamentary structures within a protein rich biological matrix. The intrinsic colloidal environment supports filament stabilisation and coupling to structured domains without the need for external templating or crystallisation.

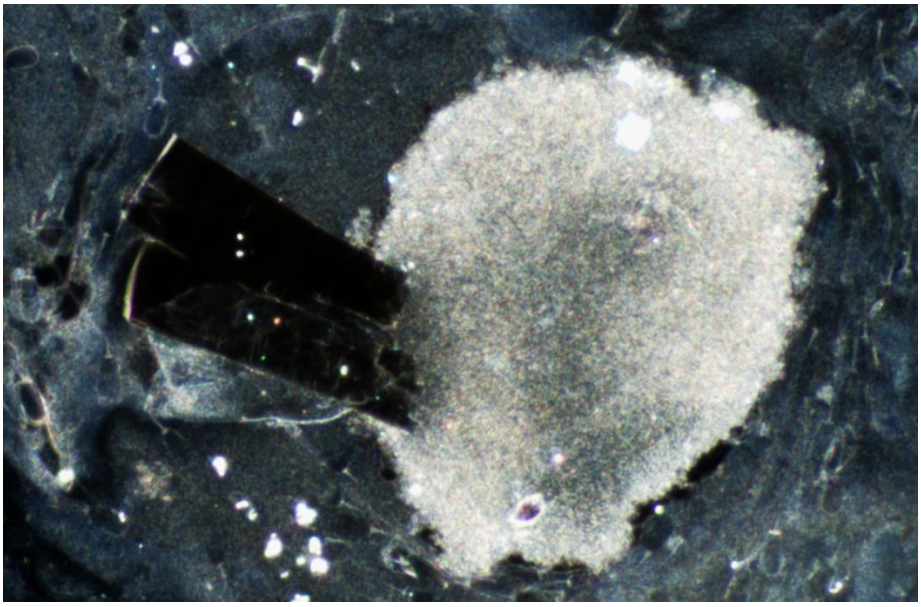

Figure 39. Dense phase-separated aggregate within a protein-rich biological fluid, showing a sharply bounded condensation adjacent to a dark, angular inclusion. Magnification 400x.

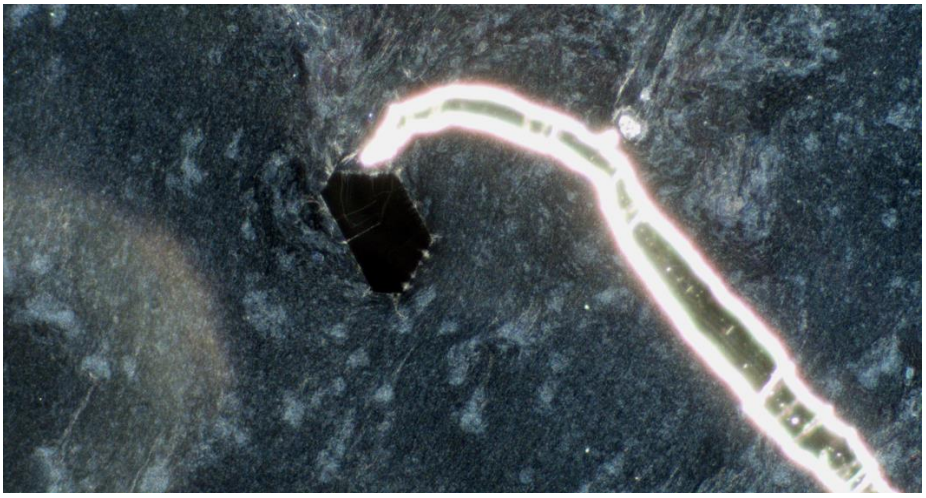

Figure 40. Dark-field image showing a non-orthogonal, irregularly faceted crystalline inclusion adjacent to a continuous filament within a sedimented biological matrix. The crystalline body departs from classical square or rectangular symmetry and exhibits asymmetric geometry, while the adjoining filament maintains optical continuity along its length. The interface suggests local coupling between crystalline and filamentary phases rather than independent crystallisation. Magnification 400x.

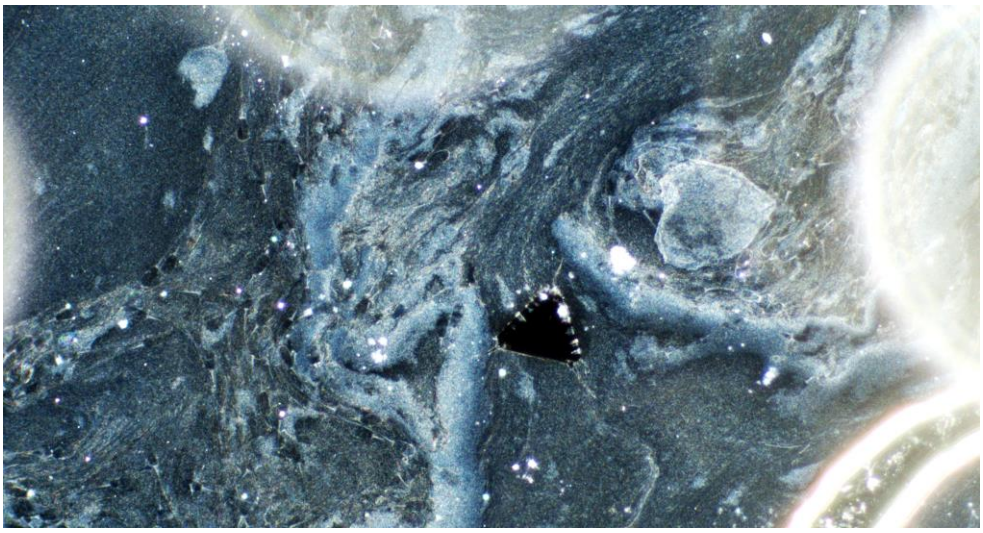

Figure 41. Dark-field image of an irregular, triangular crystalline inclusion embedded within a protein-rich biological matrix. The crystal exhibits non-orthogonal geometry and sharp faceting, with an adjacent hydrogel-like region visible at the lower right margin. Surrounding material shows diffuse particulate sedimentation without organised lattice formation. Magnification 200x.

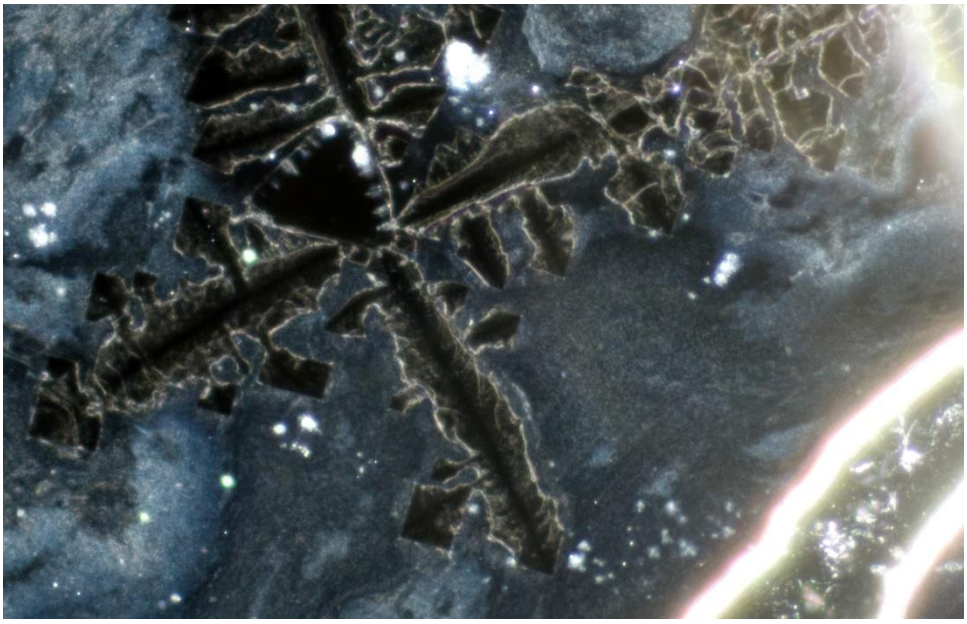

Figure 42. Dark-field image of the same field one week later. The previously isolated triangular crystalline inclusion is now centrally positioned within a dense sedimentary lattice. Rectilinear, templated structures have emerged at the periphery of the crystal, forming angular extensions aligned with its facets. The surrounding matrix appears more structured, with organised sedimentation replacing the earlier diffuse background. Magnification 400x.

Taken together, Figures 38 and 39 document a time-dependent reorganisation of the surrounding matrix centred on a pre-existing crystalline inclusion. An initially isolated, irregular crystal associated with a hydrogel-like phase becomes, over the course of one week, the focal point for structured sedimentation and the emergence of rectilinear forms aligned to its geometry. This progression suggests that crystallisation alone is insufficient to explain the observed architecture, and that persistent crystalline domains can act as organising centres for subsequent phase-mediated patterning within biological fluids.

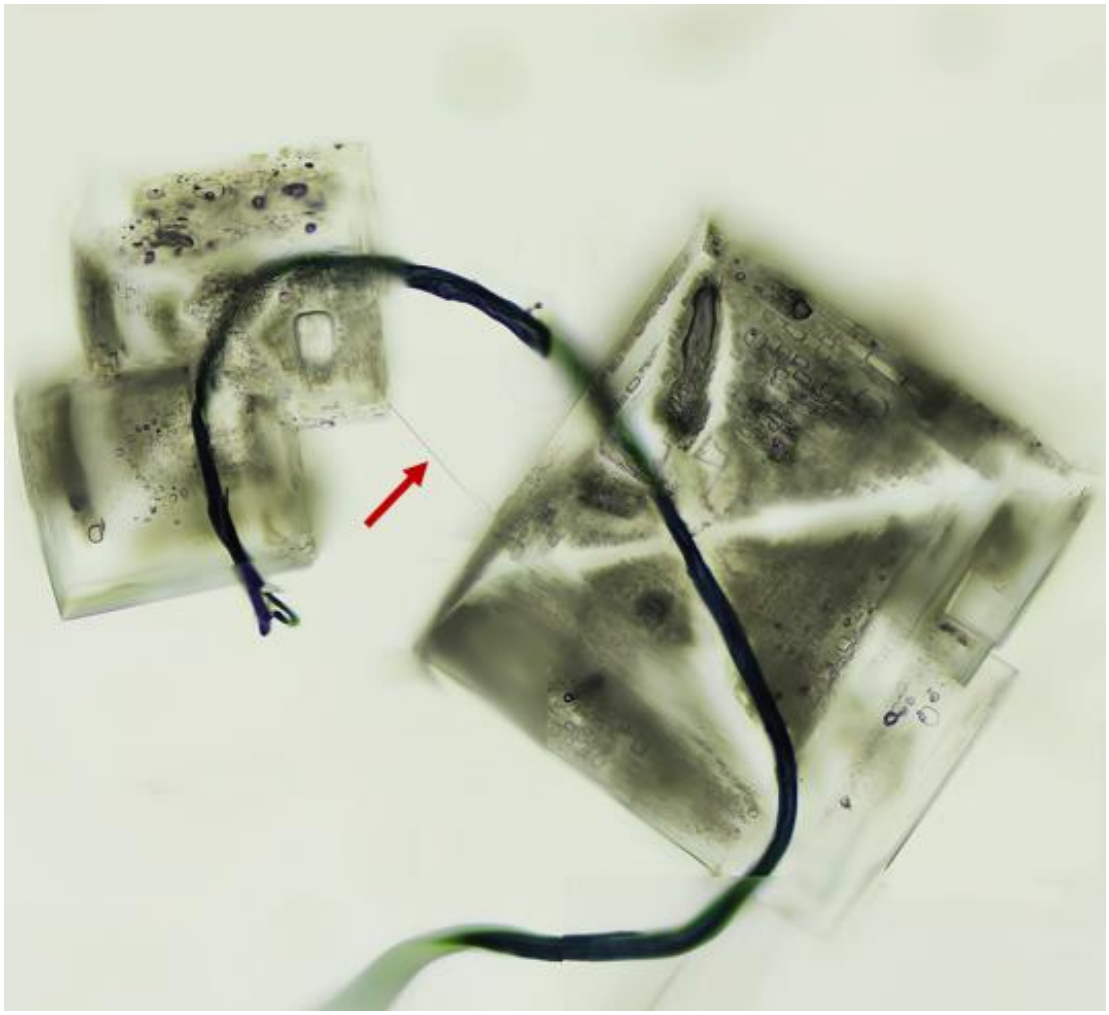

Figure 43. Independent reproduction of a Crystal–Fibre Assembly showing two rectilinear crystalline domains coupled by a continuous curved fibre. The fibre maintains optical continuity between crystals and exhibits directed curvature rather than random alignment. Internal patterning and edge coherence are conserved across both crystalline bodies. Image provided by an independent collaborator following minimal methodological guidance. Magnification 200x

Figure 40 shows an independently prepared sample incorporating a commercially available C60-containing supplement, coverslip confinement, photo-stitched imaging, and overnight incubation at 37 °C produced a highly resolved Crystal–Fibre Assembly exhibiting multi-crystal coupling via a continuous curved filament.

Despite substantial differences in preparation conditions and material composition, the resulting architecture preserved the defining features of CFAs observed elsewhere in this study, including rectilinear crystalline geometry, internal patterning, and fibre-mediated spatial linkage across discrete domains.

This observation demonstrates that CFA formation is not restricted to a narrow set of formulations or protocols, but can emerge under conditions that enhance structural stabilisation, boundary definition, and temporal maturation.

Bridging dark-field and phase-contrast observations

The region indicated by the red arrow marks the point of apparent fibre–crystal interface as visualised under dark-field illumination, where the filament appears to terminate or enter the crystalline boundary. In dark-field imaging, this junction presents as a zone of high optical contrast, suggesting close spatial coupling but offering limited insight into internal structure. Phase-contrast imaging of the same assembly reveals additional organisation at this interface, resolving an internal, longitudinal void or channel within the crystalline domain that aligns with the incoming fibre.

This correspondence between dark-field and phase-contrast views indicates that the apparent boundary interaction observed under dark-field conditions reflects a deeper structural integration, in which the fibre is accommodated within an internal crystalline feature rather than merely abutting the crystal surface.

Taken together, these complementary modalities support interpretation of the assembly as an integrated crystal–fibre architecture with internal continuity, rather than a superficial or post hoc association.

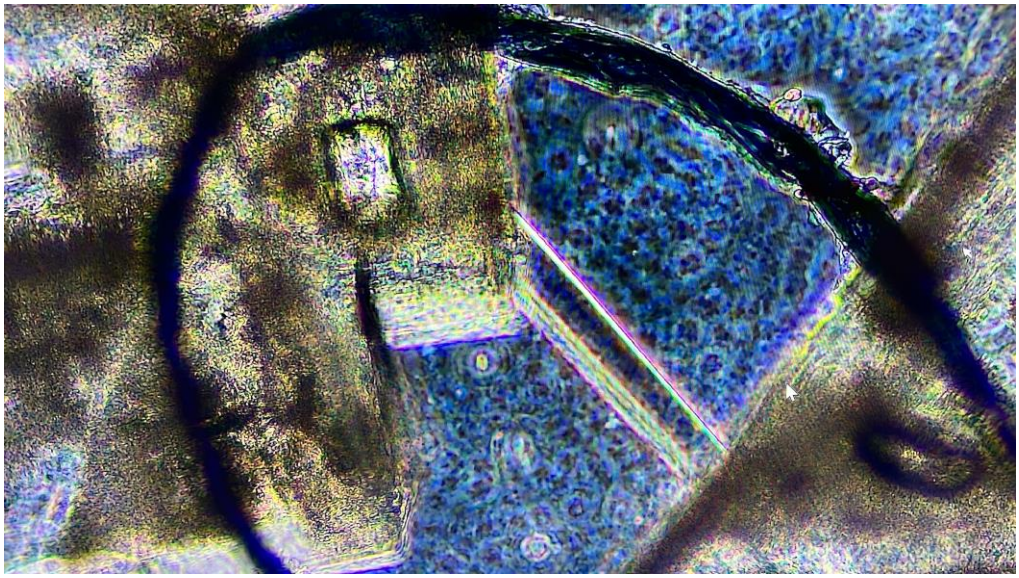

Figure 44. Phase-contrast image of a crystal–fibre assembly showing a fibre entering a rectilinear crystalline domain at an oblique angle. An internal longitudinal void or channel is visible within the crystal, aligned with the incoming fibre. The correspondence between fibre trajectory and internal crystalline feature suggests structural integration at the interface rather than superficial contact. Magnification 400x.

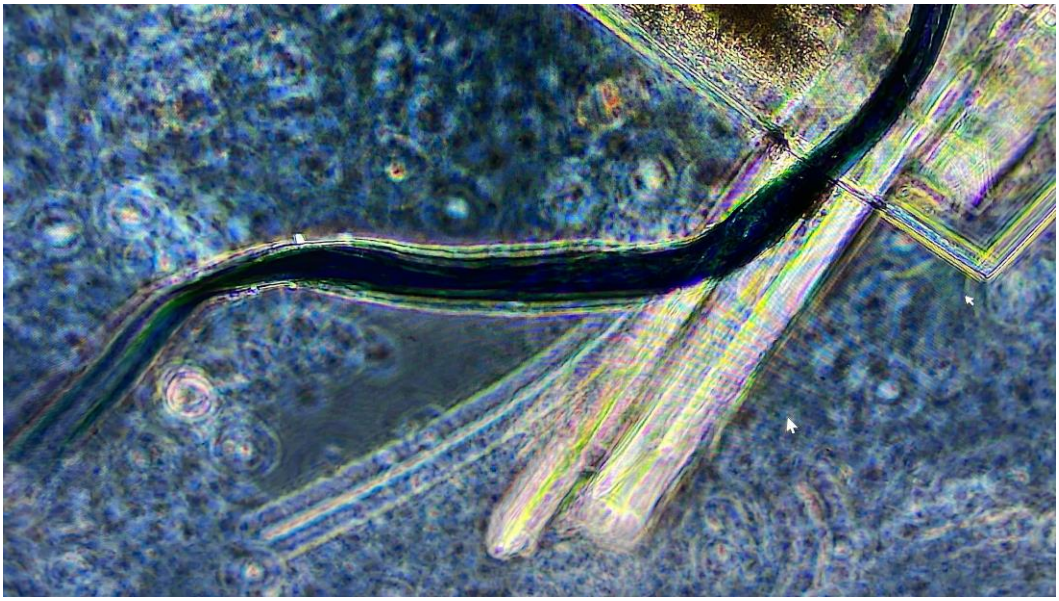

Figure 45. Phase-contrast image showing a linear crystalline protrusion emerging directly from the lower face of a larger rectilinear crystal. The protruding element exhibits uniform thickness, straightness, and geometric continuity with the parent crystal, forming a rigid linear extension rather than a tapered or fragmented outgrowth. This configuration is consistent with internally constrained directional growth or phase-coupled extrusion. Magnification 500x

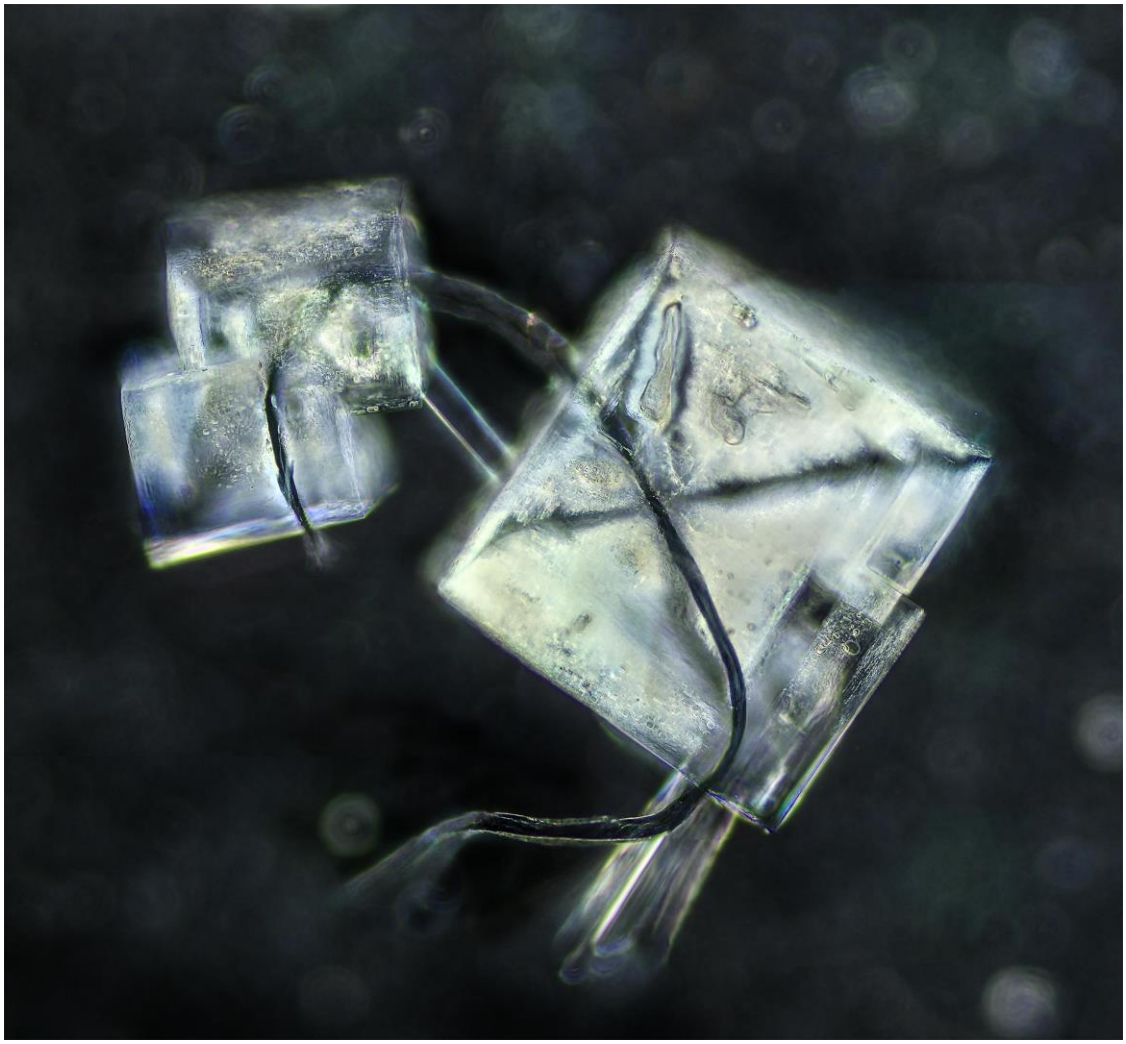

Figure 46. Dark field. Photo-stitched composite showing two rectilinear crystalline domains coupled to a dark fibre. In the larger crystal, the fibre forms a continuous track across the crystalline interior and exits the lower face as an uninterrupted filament. Linear rod-like crystalline protrusions are present beneath the larger crystal, aligned with the exiting fibre. Magnification 100x.

Phase-contrast imaging further revealed that the apparent fibre termination observed under dark-field illumination corresponded to a hollow or channel-like internal structure within the crystalline body, indicating internal continuity rather than external attachment.

Results Summary (Crystal–Fibre Assemblies)

Across multiple pharmaceutical preparations— including Pfizer-BioNTech Comirnaty, Moderna COVID-19 vaccine, influenza vaccine, dental and non-dental anaesthetics, and budesonide — and in biological samples including blood and other protein-rich bodily fluids (urine, saliva, nasal secretions, and semen), a consistent class of Crystal–Fibre Assemblies (CFAs) was observed. These assemblies are characterised by predominantly square or rectilinear crystalline bodies exhibiting structured spatial relationships with adjacent fibres.

While fibres were not always visibly continuous through the crystalline volume under a single imaging modality, complementary imaging demonstrated internal continuity, channelling, or phase-aligned incorporation in several cases. This striking consistency of geometry, alignment, and positional coupling was maintained across samples, preparations, and timepoints.

In several instances, fibres traversed crystalline domains without interruption, acted as shared axes linking multiple crystals, or extended beyond crystal boundaries as continuous elements. In other cases, fibres and crystals remained spatially distinct yet exhibited coordinated orientation, curvature, or synchronous development, suggesting coupling within a shared formation domain despite the absence of direct continuity. Time-lapse observations further demonstrated coordinated maturation of crystalline nodes along individual fibres, preservation of spatial memory, and repeated emergence of comparable motifs under distinct experimental conditions.

Taken together, these findings are not consistent with classical heterogeneous nucleation, incidental surface contact, or random post-hoc mechanical interaction. Instead, the reproducibility of form, alignment, and developmental behaviour — regardless of whether direct fibre continuity is present — supports the interpretation of a phase-coupled organisational process operating within the crystallisation field. These results establish CFAs as a reproducible structural class across pharmaceutical formulations and blood samples, providing a coherent empirical foundation for subsequent discussion of coherence-dependent self-assembly, field sensitivity, and non-local organisational dynamics.

Discussion

Across the diverse sample types examined in this study, a recurring structural motif was observed in the form of coupled crystalline and fibrous architectures, herein referred to as Crystal–Fibre Assemblies (CFAs). These structures appeared across chemically and functionally distinct domains, including mRNA vaccines, dental and non-dental anaesthetics, inhaled corticosteroid solutions, blood, and urine. Their repeated emergence under varied conditions argues against isolated artefact, contamination, or domain-specific anomaly, and instead points toward a shared organisational tendency operating across soft matter systems.

Importantly, CFAs were not defined by chemical composition alone. Rather, they reflect a phase-dependent organisational logic in which crystalline domains and fibrous elements coexist, interact, and in some cases undergo coordinated transformation within a shared assembly regime. This observation supports a framework in which structural behaviour is governed less by molecular identity and more by boundary conditions such as evaporation dynamics, confinement, ionic environment, and exposure to external fields. In this sense, CFAs should be understood not as fixed entities but as transient or stabilised intermediates within a broader self-assembly landscape.

The results presented here require a refinement of how crystal–fibre relationships are interpreted. While some assemblies demonstrate uninterrupted fibre continuity through crystalline bodies, others preserve consistent geometry, alignment, and spatial coupling despite apparent physical discontinuity. This indicates that fibre continuity is not a prerequisite for coordinated assembly.

Phase-contrast observations indicate that apparent discontinuity under dark-field imaging may reflect optical limitation rather than true structural separation, with fibres in some cases accommodated within internal crystalline channels. Instead, the defining feature of Crystal–Fibre Assemblies lies in the preservation of form, orientation, and developmental logic across spatial gaps. Such behaviour is inconsistent with classical heterogeneous nucleation or incidental post-formation contact and instead points to organisation within a shared phase domain.

The recurrence of these structures across distinct pharmaceutical formulations—including mRNA vaccines, influenza vaccines, dental and non-dental anaesthetics—and within blood samples further argues against formulation-specific artefact. Rather than isolated chemical events, these assemblies appear to reflect a generic organisational capacity of certain soft-matter systems to couple crystalline growth with fibre-aligned structuring. In this context, fibres function not merely as physical scaffolds but as phase-participating elements capable of coordinating structure across distance within the crystallisation field.

Notably, the expression of CFA-related structures varied by domain. In pharmaceutical preparations, particularly vaccines and anaesthetic solutions, crystal–fibre coupling was commonly observed, often emerging during sessile droplet evaporation or incubation. In contrast, blood samples predominantly exhibited fibrous and vesicular architectures, with crystalline elements notably rare. Only a single CFA-like structure was observed under blood-derived conditions, and this occurred under atypical conditions involving prolonged incubation and proximity to a magnetic field. Urine samples occupied an intermediate position, showing evidence of persistent structured material but with variable crystallinity. These differences suggest that local environmental constraints — including protein content, flow, hydration state, and biological buffering — strongly influence whether crystalline phases are permitted, suppressed, or transformed.

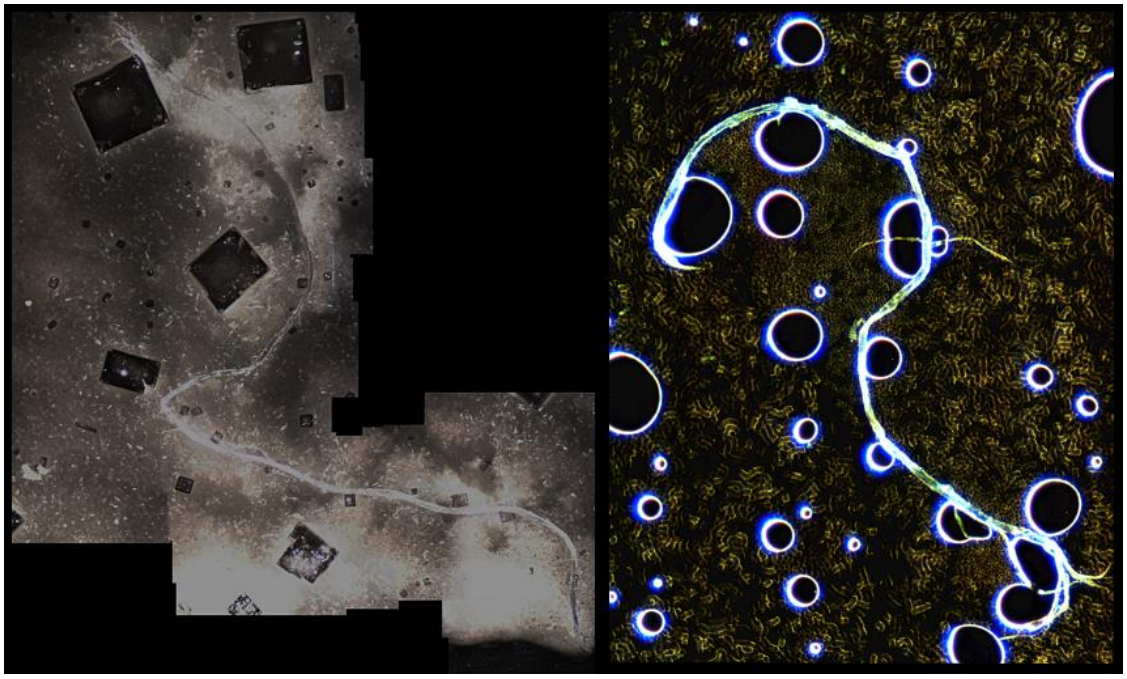

Figure 47. On the left, a photo-stitched view of crystalline domains coupled to a fibre in a 2-month-old Pfizer Comirnaty sample. On the right, a fibre-like structure associated with vesicular domains in a 10-minute-old blood sample. Both images were acquired at approximately 40× magnification.

The sensitivity of these structures to boundary conditions is a critical finding. Changes in evaporation rate, confinement (such as the use of coverslips), and field exposure were associated with altered structural outcomes. This responsiveness reinforces the interpretation of CFAs as dynamic architectures rather than passive residues. In this context, the presence of fibrous networks coupled to vesicles or crystalline domains may represent a generalised soft matter response to gradients and constraints, rather than evidence of intentional design or discrete agents.

The implications of these observations are primarily epistemological and methodological. If structurally active materials can arise through phase logic alone, then risk assessment frameworks that rely exclusively on chemical identity or concentration may be insufficient. Structural behaviour — including the capacity to self-organise, persist, or respond to environmental triggers — becomes a relevant dimension of analysis. This does not imply biological harm per se, nor does it assert causality with clinical outcomes. Rather, it highlights a category of material behaviour that is currently under-recognised in biomedical and pharmaceutical evaluation.

Observations made at the periphery of blood samples following prolonged proximity to a static magnetic field further support the interpretation of CFAs as phase-coupled rather than contact-driven structures. While magnetic exposure cannot be isolated as a causal factor in the present study, the preservation of fibre–crystal alignment and continuity under these conditions suggests sensitivity to external field gradients rather than random mechanical interaction.

These findings reinforce the need to consider environmental and field-dependent influences when interpreting microscale self-assembly in biological fluids. Recent phase-contrast observations further indicate that linear crystalline extensions may emerge directly from parent crystalline bodies along fibre-aligned axes, reinforcing the interpretation of CFAs as internally coordinated, phase-coupled architectures rather than surface-mediated contacts.

Several limitations must be acknowledged. This study is observational and microscopy-based, and it does not attempt to establish biological mechanisms, toxicity, or physiological impact. Sample sizes are limited, and the work prioritises structural documentation over quantitative analysis. Nonetheless, the reproducibility of CFA-like motifs across domains and contexts provides a coherent basis for further investigation.

In summary, the recurrence of Crystal–Fibre Assemblies across pharmaceuticals and biological fluids suggests the operation of a shared, phase-dependent organisational logic within soft matter systems. Recognising and characterising such structures may be essential for developing a more complete understanding of material behaviour at the interface of chemistry, biology, and environment.

Conclusion

This study documents the recurrent emergence of Crystal–Fibre Assemblies (CFAs) across multiple pharmaceutical and biological domains. Observed in vaccines, anaesthetics, inhaled medications, urine, and under limited conditions in blood, these structures exhibit consistent organisational features despite substantial differences in

chemical formulation and biological context. Their recurrence suggests that CFAs are not isolated artefacts but expressions of a shared phase-dependent structural logic.

The findings indicate that fibrous architecture, with crystallinity and vesicle coupling as conditional expressions, arises or is suppressed according to local boundary conditions rather than fixed material identity.

In environments such as blood, where flow, buffering, and biological regulation dominate, fibrous and vesicular forms predominate, with crystallisation largely constrained. In contrast, pharmaceutical and excretory contexts permit more overt crystal–fibre coupling. This differential expression reinforces the interpretation of CFAs as environmentally mediated structures rather than static inclusions.

Importantly, this work does not claim biological harm, intent, or clinical consequence. Its contribution lies in demonstrating that structurally persistent, responsive architectures can arise across domains traditionally treated as chemically inert or transient. By foregrounding structure, phase behaviour, and environmental sensitivity, the study highlights a gap in existing analytical frameworks that prioritise composition while overlooking dynamic organisation.

Taken together, these observations support the need for further investigation into phase-coupled soft matter behaviour in biomedical contexts. Establishing when, where, and under what conditions such structures arise — and how they are differentially revealed by imaging modality — is a necessary precursor to assessing their relevance within biological systems.

References

Ayrapetyan, S. N., & Ayrapetyan, G. S. (2010). Cell hydration and metabolism: Implications for electromagnetic field effects. In M. Markov (Ed.), *Electromagnetic Fields in Biology and Medicine* (pp. 75–94). CRC Press.

Del Giudice, E., Doglia, S., Milani, M., & Vitiello, G. (1986). Electromagnetic field and spontaneous symmetry breaking in biological matter. *Nuclear Physics B*, 275(2), 185–199.

Del Giudice, E., Doglia, S., Milani, M., Vitiello, G., & Vitale, M. (1989). Magnetic flux quantisation and Josephson behaviour in living systems. *Physica Scripta*, 40(6), 786–791. https://doi.org/10.1088/0031-8949/40/6/017

Del Giudice, E., Voeikov, V., Tedeschi, A., & Vitiello, G. (2015). The origin and the special role of coherent water in living systems. In L. Montagnier, J. Aïssa, E. Del Giudice, & G. Vitiello (Eds.), *Fields of the Cell* (pp. 77–92). World Scientific. https://doi.org/10.13140/RG.2.1.2329.1046

Nixon, D. (2025a). *Active microscale construction in Pfizer Comirnaty: A live microscopy study*. *Journal of Bionanotechnocracy: Countdown to 2030*, 1(1), 1–112. https://www.journalbnt.org

Nixon, D. (2025b). *Nano makes micro: Emergent structural logic across pharmaceutical and biological systems*. *Journal of Bionanotechnocracy: Countdown to 2030*, 1(1), 113–197. https://www.journalbnt.org

Nixon, D. (2025e). *Self-assembling nanostructures in blood and urine: Implications for bioaccumulation and detoxification*. *Journal of Bionanotechnocracy: Countdown to 2030*, 1(1), 279–312. https://www.journalbnt.org

Nixon, D. (2025f). *Coherence-dependent self-assembly in dental anaesthetics: Structural modulation through passive field exposure*. *Journal of Bionanotechnocracy: Countdown to 2030*, 1(1), 313–396. https://www.journalbnt.org

Nixon, D. (2025f, Appendix). *Independent confirmation of field-sensitive crystallisation through Wi-Fi modulation (Mateo Taylor contribution)*. Appendix in *Coherence-dependent self-assembly in dental anaesthetics*. *Journal of Bionanotechnocracy: Countdown to 2030*, 1(1), 313–396. https://www.journalbnt.org

Nixon, D. (2025g). *From captured coherence to structural reversal: Field-modulated self-assembly in dental anaesthetics and blood*. *Journal of Bionanotechnocracy: Countdown to 2030*, 1(2), 397–432. https://www.journalbnt.org

Nixon, D., Wade, W. (2025h). *Multi-modal microscopy of coherence disruption: Orgonite, Trivortex, light and electromagnetic shielding in pharmaceutical samples*. *Journal of Bionanotechnocracy: Countdown to 2030*, 1(2), 433–468. https://www.journalbnt.org

Nixon, D., Beharrell, T. (2025i). *Phase-dependent structural transformation of hydrogel-like materials across pharmaceutical and biological contexts.* Journal of Bionanotechnocracy: Countdown to 2030, 1(2), 504–526. Retrieved from https://www.journalbnt.org

Nixon, D. (2026a). *From Hydrogel to Metamaterial: Redefining Structural Behaviour in Pharmaceutical and Biological Fluids*. Journal of BioNanoTechnocracy, 2(1), 115–139. www.journalbnt.org

Pollack, G. H. (2013). *The fourth phase of water: Beyond solid, liquid, and vapor*. Ebner & Sons.

Pujala, R. K., Sudhakaran, D. V., & Dhara, S. (2020). Evaporation-driven self-assembly in mixtures of micro- and nanoparticles. *Bulletin of Materials Science*, 43(1), 1–8. https://doi.org/10.1007/s12034-020-02096-5

Youssef, M., Hueckel, T., Yi, G.-R., & Sacanna, S. (2016). Shape-shifting colloids via stimulated dewetting. *Nature Communications*, 7, 12216. https://doi.org/10.1038/ncomms12216

Zang, S., Paul, S., Leung, C. W., Chen, M. S., Hueckel, T., Hocky, G. M., & Sacanna, S. (2025). Direct observation and control of non-classical crystallisation pathways in binary colloidal systems. *Nature Communications*, 16, 3645. https://doi.org/10.1038/s41467-025-58959-0

Conflict of Interest Statement

This research was conducted independently, with no external influences affecting the data or conclusions presented. While some income is derived from subscriptions to my personal *Substack* publication, this does not compromise the integrity or objectivity of the study. No other conflicts of interest are reported. This work has been entirely privately funded.

Copyright Notice

For additional materials, images, and videos, please visit:

http://www.drdavidnixon.com

Glossary

Architectural Motif
A reproducible structural pattern defined by spatial organisation and relational geometry, recurring across samples and domains independent of composition.

Boundary Conditions
The environmental, geometric, or energetic constraints (e.g. evaporation rate, confinement, field exposure) that permit or suppress the emergence of CFAs.

Capillary Flows
Fluid movements within an evaporating droplet driven by surface tension gradients, influencing particle redistribution and structural alignment.

Colloidal Particles
Microscale or nanoscale particles suspended within a fluid that act as intermediates in self-assembly processes, linking nano- and microscale organisation.

Crystal–Fibre Assembly (CFA)
A recurring structural motif characterised by a persistent architectural coupling between a crystalline domain and one or more fibre-like elements. CFAs are defined by geometry and organisation rather than chemical composition and are observed across pharmaceutical and biological contexts.

Dark Field Microscopy (DFM)
A microscopy technique that enhances contrast in transparent samples by collecting scattered light, enabling visualisation of fine structures not visible under bright field illumination.

Dynamic Self-Assembly
The spontaneous organisation of components into structured formations through continuous movement, adaptation, and reorganisation over time.

Encapsulation Events
The formation of closed or semi-closed boundaries around fibres or crystalline cores during self-assembly, suggesting active material organisation.

Fractal Stratification
Layered, scale-recursive organisation within self-assembled structures, where similar geometric features repeat across magnifications.

Hierarchical Organisation
Structural organisation spanning multiple spatial scales, with nested or repeating features linking nano- and microscale domains.

Hydrodynamic Flow
The movement of liquid within a system that affects spatial organisation and alignment of assembling components.

Nano Makes Micro
A principle describing how nanoscale components aggregate and organise into observable microscale structures through self-assembly.

Nested Assembly Architecture
The recursive formation of organised substructures within larger assemblies, reflecting templated or constrained assembly logic.

Non-Classical Crystallisation
Crystallisation processes that deviate from simple ion-by-ion growth, often involving intermediates such as colloids, vesicles, or fibres.

Nucleation
The initial clustering of particles or molecules that seeds subsequent growth of a crystalline or organised structure.

Phase-Coupled Architecture
A structural configuration whose formation and persistence depend on coordinated transitions between material phases (e.g. vesicular, fibrous, crystalline).

Phase Transitions
Changes in material organisation or state, such as liquid-to-solid or amorphous-to-crystalline, that influence self-assembly behaviour.

Reversible Assembly
The capacity of structures to assemble, partially disassemble, and reconstitute in response to changing environmental conditions.

Sessile Droplet Evaporation (SDE)
An analytical method in which a liquid droplet evaporates on a substrate under ambient conditions, revealing capillary flows, phase transitions, and self-assembly dynamics.

Structural Motif Recurrence
The repeated appearance of the same organised architecture across independent samples, magnifications, and domains.

Surface Tension Dynamics
The role of interfacial forces in shaping particle motion, aggregation, and pattern formation during evaporation.

Vesicle-Like Structures
Spherical or membrane-bounded formations observed during SDE, often interacting dynamically with fibres or crystalline domains.

Vesicle-to-Rod Transition
A dynamic process in which vesicular structures elongate into rod- or fibre-like forms, often preceding crystalline nucleation or boundary formation.

Legal Disclaimer